Direct-Detection Spectroscopy with CCAT

C. M. Bradford
with
J. Zmuidzinas, J. Glenn, T. Nikola, G. Stacey

December 13, 2006

Topics

- Scientific motivation for terrestrial submillimeter spectroscopy.
  (extragalactic: local universe and redshift > 1).
- Sensitivities of CCAT for spectroscopy, context with ALMA & pending flight opportunities.
- Areal and redshift density of high-z sources accessible via C+ with CCAT.
- Optimal spectrometer choices, relationships to present-day instruments.
- Instrument scope, detector options, cost.

Introduction: IR astronomy is **far**-IR astronomy

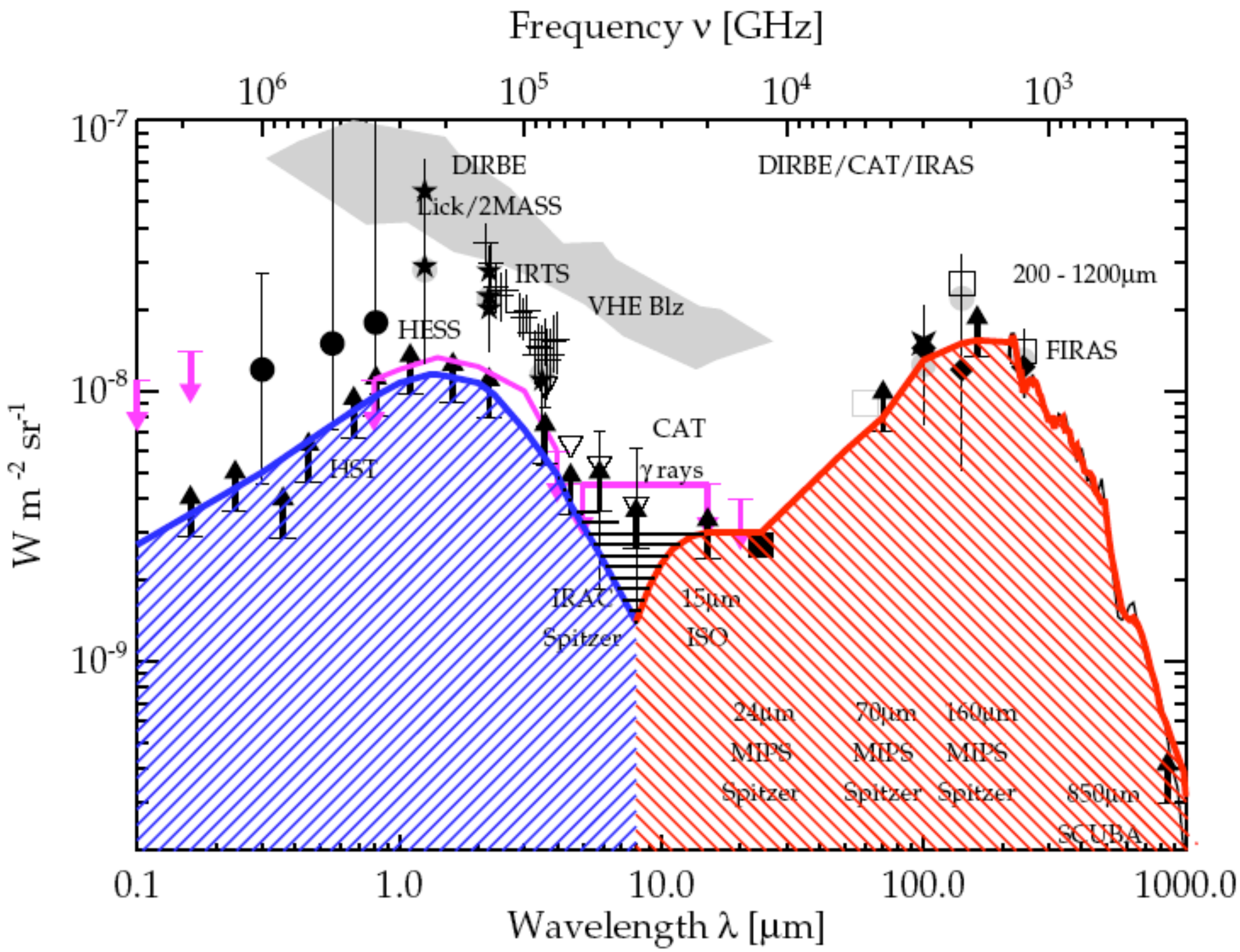

Fig. 13. Our best Cosmic Optical Background (blue-shaded, left) and Cosmic Infrared Background (red-shaded, right) estimates. The gray-shaded area represents the region of overlap. See Fig. 9 for the other symbols.

Cosmic Backgrounds
Galaxy counts +
COBE + Spitzer
(Dole et al. 2005)

- History of stars and galaxies written at both optical / NIR and far-IR wavelengths.

Questions:

What have we learned about the production of the CFIRB?

What is the relationship between the populations producing the CFIRB and the COB?

This interesting half of the luminosity has been difficult to observe

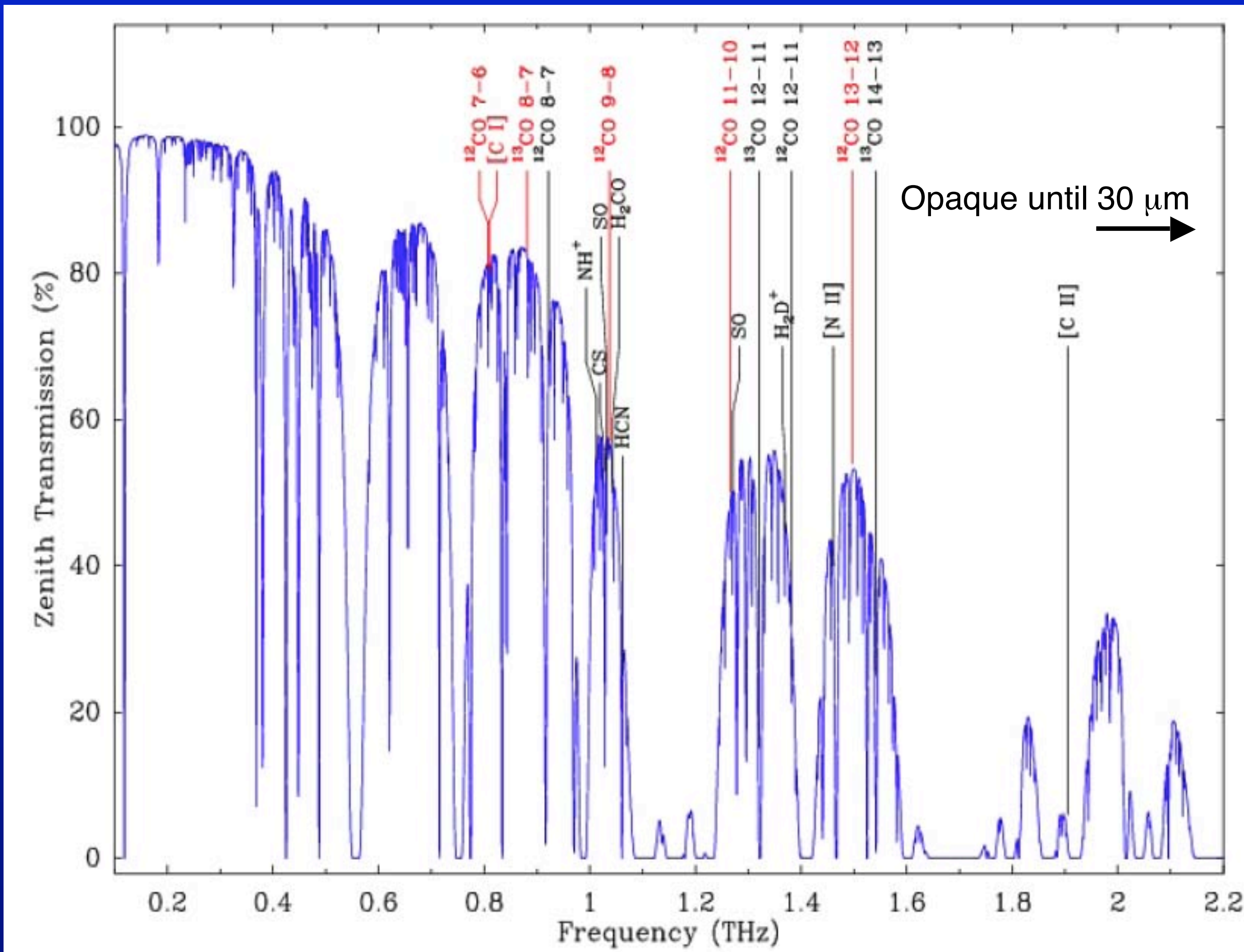

Atmosphere is opaque and warm

- Reduces transmission
- Introduces loading

-> CCAT to be at the best terrestrial site

- Far-IR /submm detector technology also behind optical / near-IR,

-> But rapidly coming of age with multi k-pix arrays

Extragalactic spectroscopy beyond 100 microns

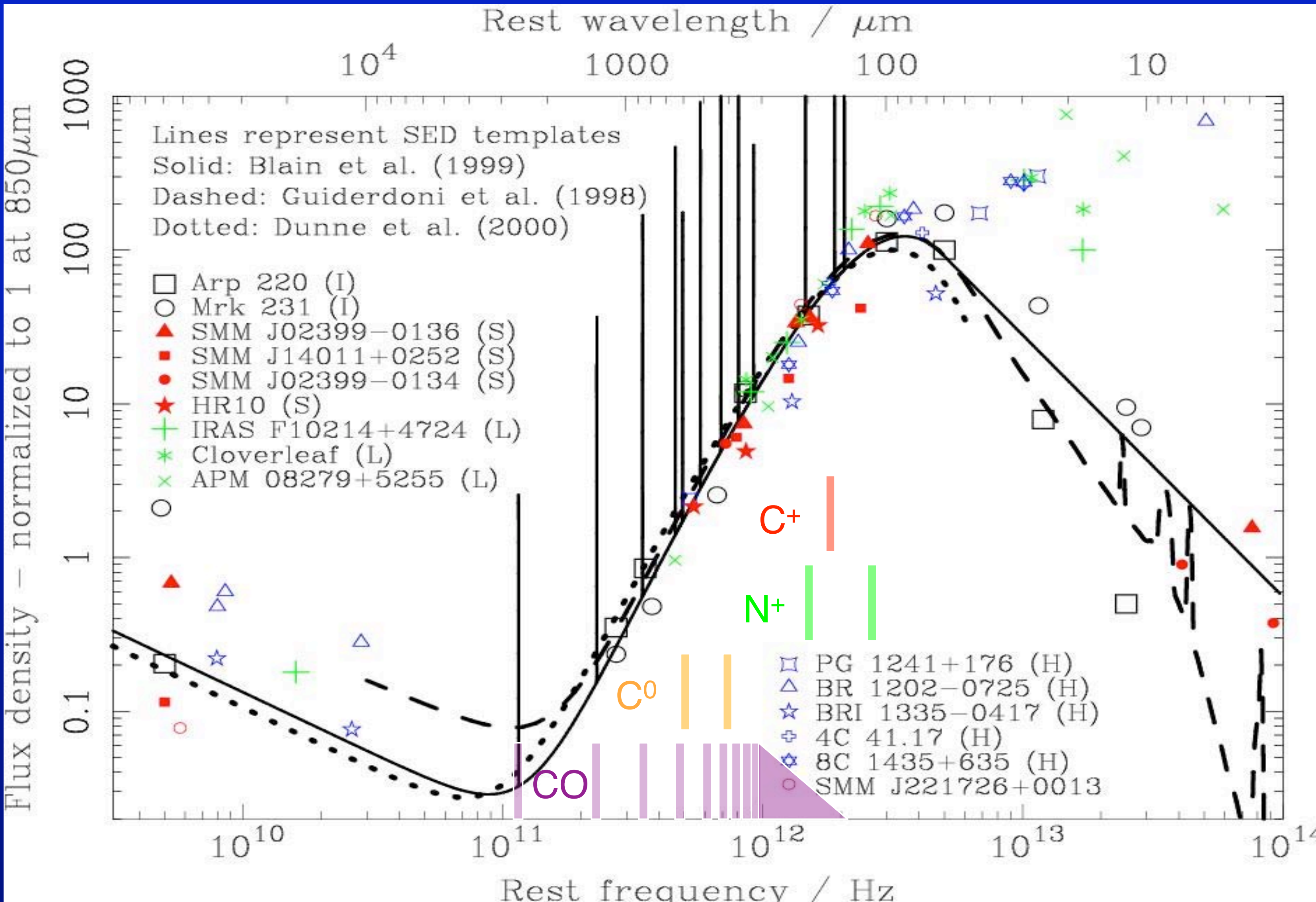

SED courtesy A. Blain

High-J CO lines: Astrophysics of the molecular gas

- LVG modeling: intensities → physical conditions
- Mid-J lines (J>4) distinguish low excitation from high excitation gas

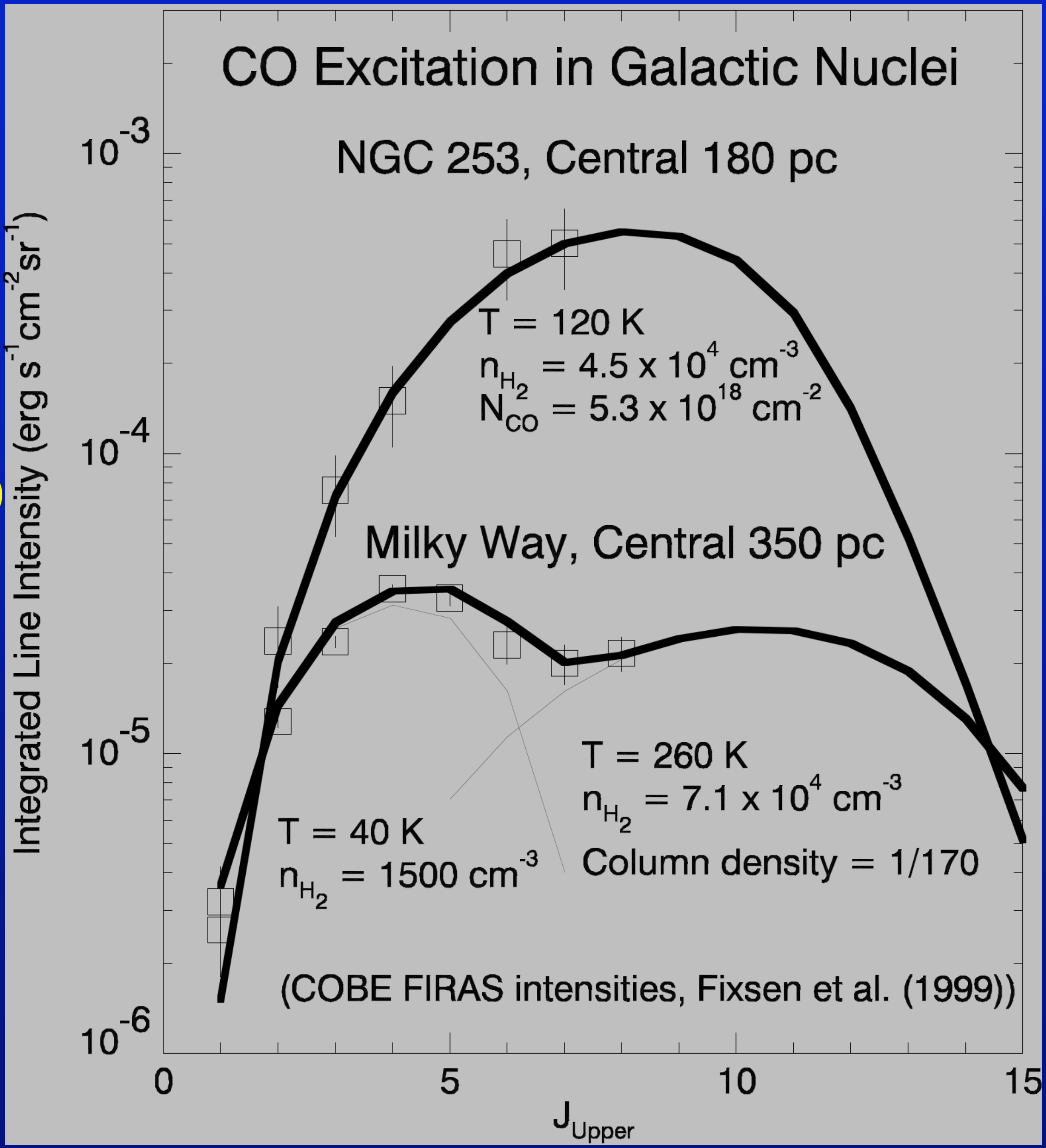

NGC 253:
Bulk of molecular gas heated to T>100 K by cosmic rays, turbulence (SPIFI – JCMT)
Bradford et al '03

Milky Way:
Mostly cool gas with small warm component from star formation regions, CND

ALMA will resolve out extended emission in nearby galaxies

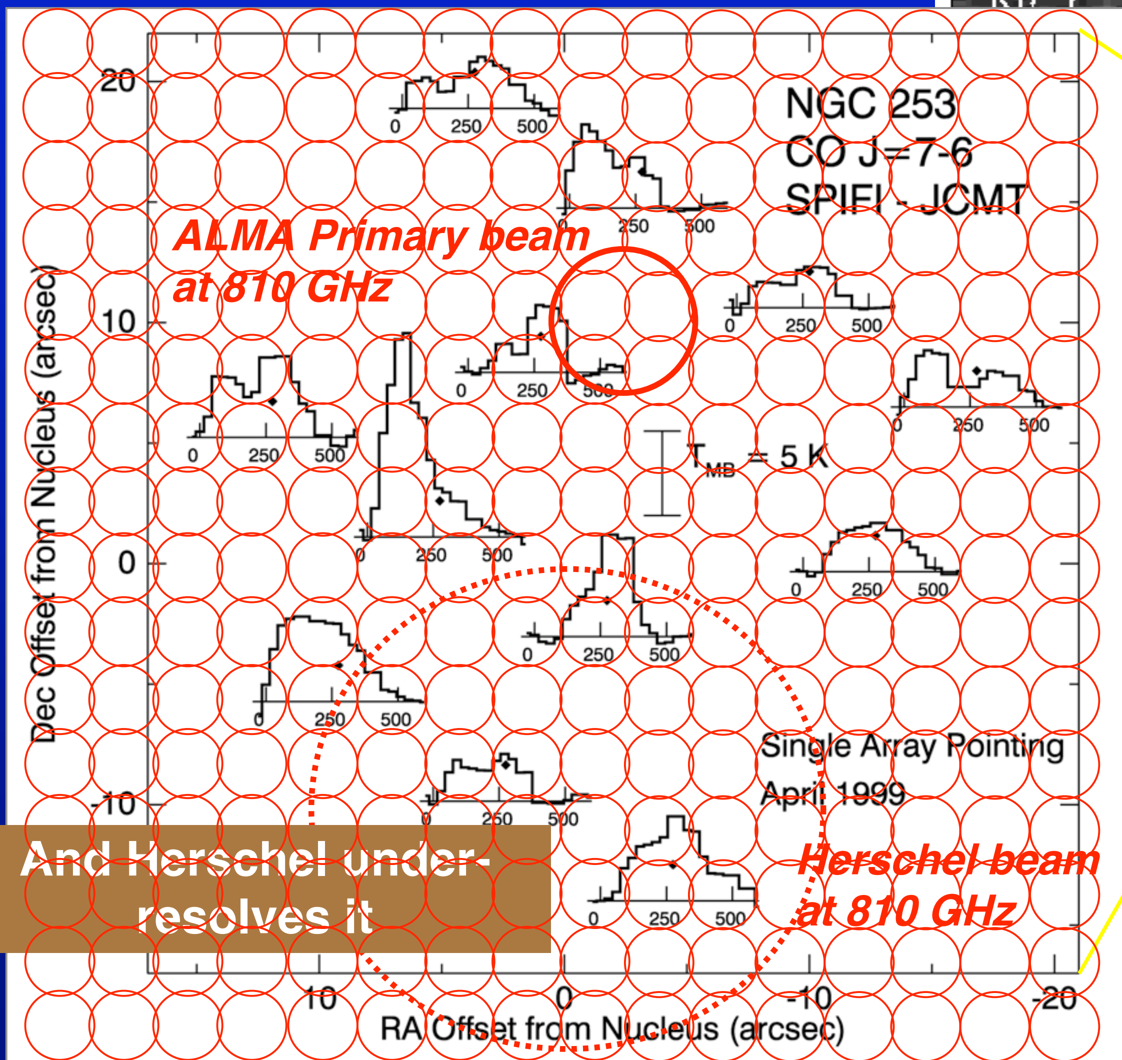

And Herschel under-resolves it

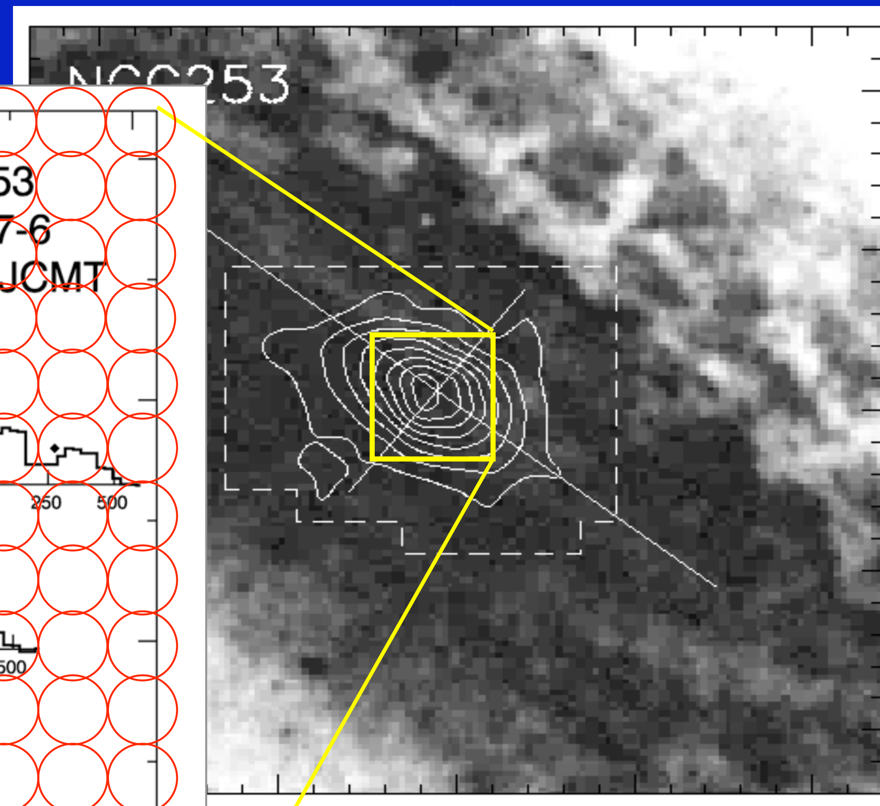

CO 3-2
M. Dumke et al. 2001,

16x16 array on CCAT

CO 7-6
Bradford et al. 2003,

CCAT can reach comfortably to redshift 0.1 for LIRGS in the CO 7-6, 6-5 and CI transitions

Far-IR background is being resolved into galaxies

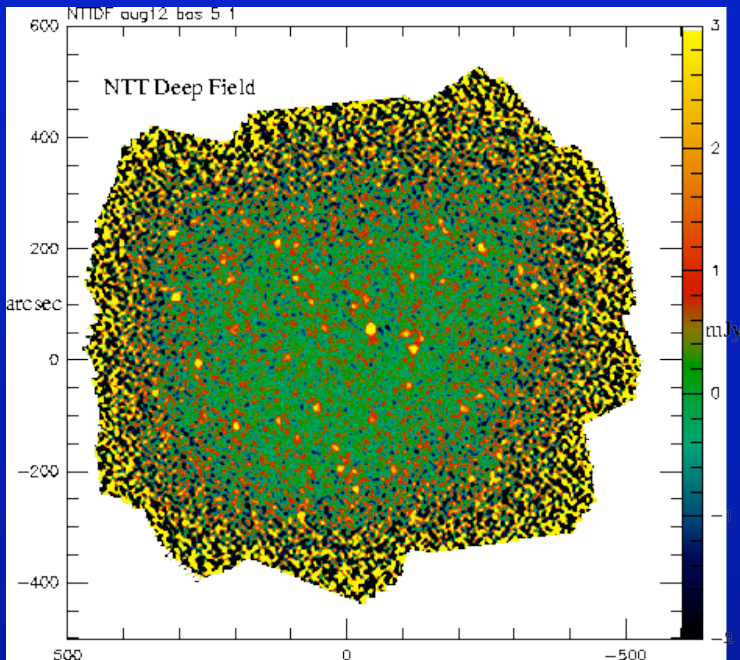

MAMBO / IRAM 30 m
1.3 mm 60 hours, 40 sources
10% of BG
Bertoldi et al. (2000);
Carilli et al. (2001c, 2002b);
Dannerbauer et al. (2002);
Voss (2002);
Eales et al. (2002)
Greve et al (2005)

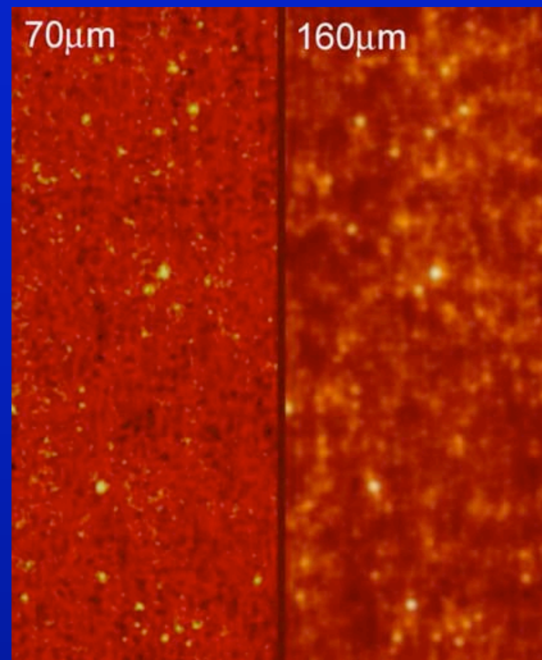

Spitzer MIPS
Chandra Deep Field South
70 (23%) 160 (7%)

Dole et al. (2004)

Dole et al. (2004)

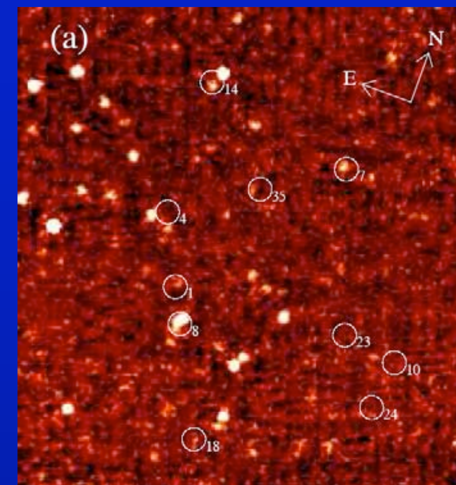

Spitzer MIPS 24 μm
Lockman Hole
Egami et al. (2004)

TABLE 3
POTENTIAL RESOLUTION OF THE COSMIC INFRARED BACKGROUND

	24 μm^a	70 μm^a	160 μm^a
Spitzer	74%	59%	18%
Herschel[b]/SPICA	98%	93%	58%
JWST[b]	99%	–	–
SAFIR	100%	99%	94%

NOTE. — (a) Using the CIB value from Lagache et al. (2004) and using the limiting flux using the SDC limit and assuming confusion-limited surveys. (b) This hypothesis might not be valid for Herschel and JWST.

Future observatories will resolve the bulk of the background into individual sources, but….
How to do meaningful follow up of these sources?
Spectroscopy with CCAT

CCAT -- redshifted fine structure lines

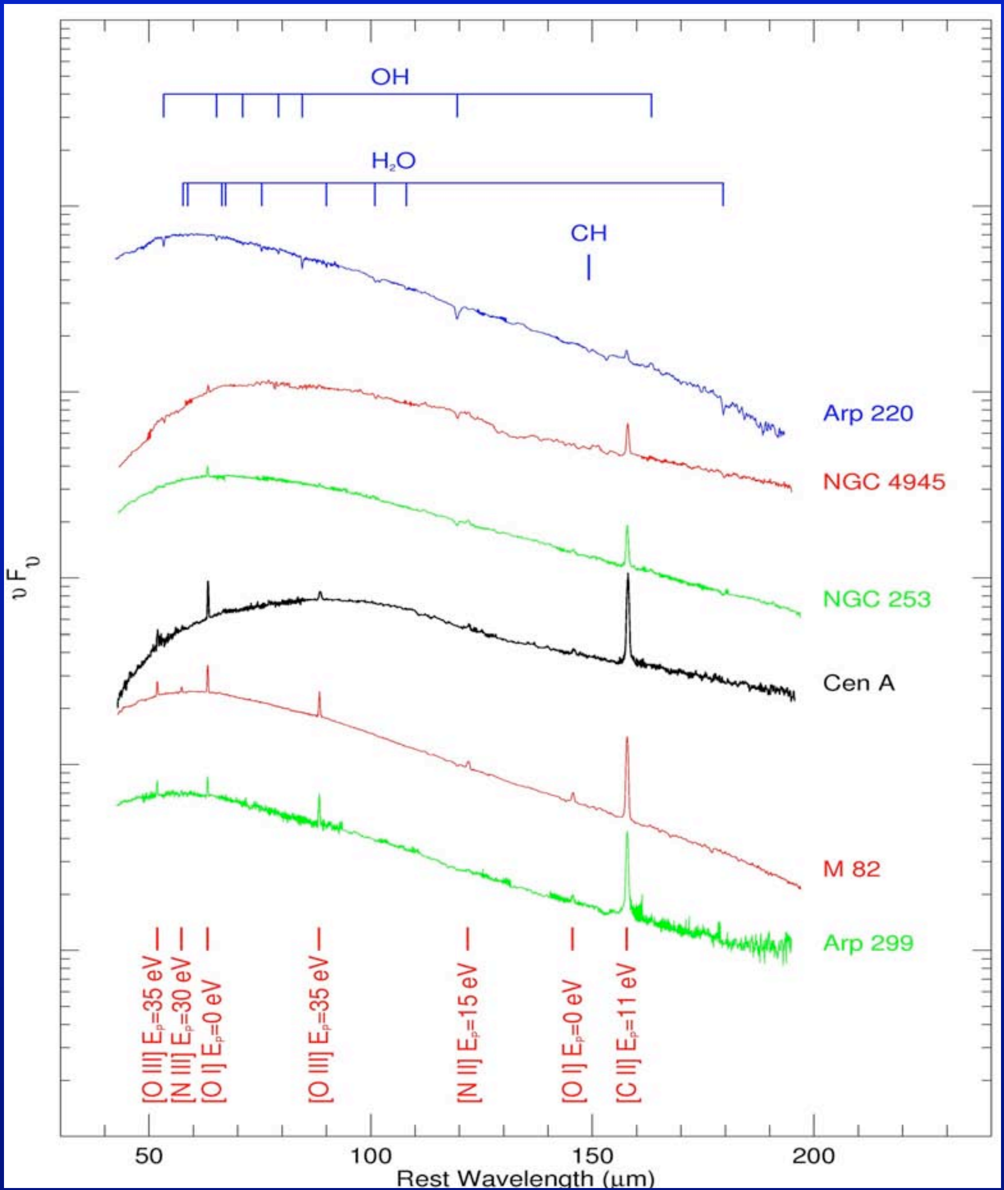

J. Fischer et al.1999

Fine structure lines probe ionized and neutral atomic gas.

→ HII region densities
→ Atomic gas pressures
→ UV field strength and hardness
→ Starburst / AGN discriminator
→ Stellar mass function

• Suite of lines is redshifted into CCAT atmospheric windows
-- provides redshift template independent of optical follow-up.

-> Also provides unique, extinction-free astrophysical probes:
UV field strength, hardness
-> stellar mass function.

CCAT Spectroscopic Sensitivities

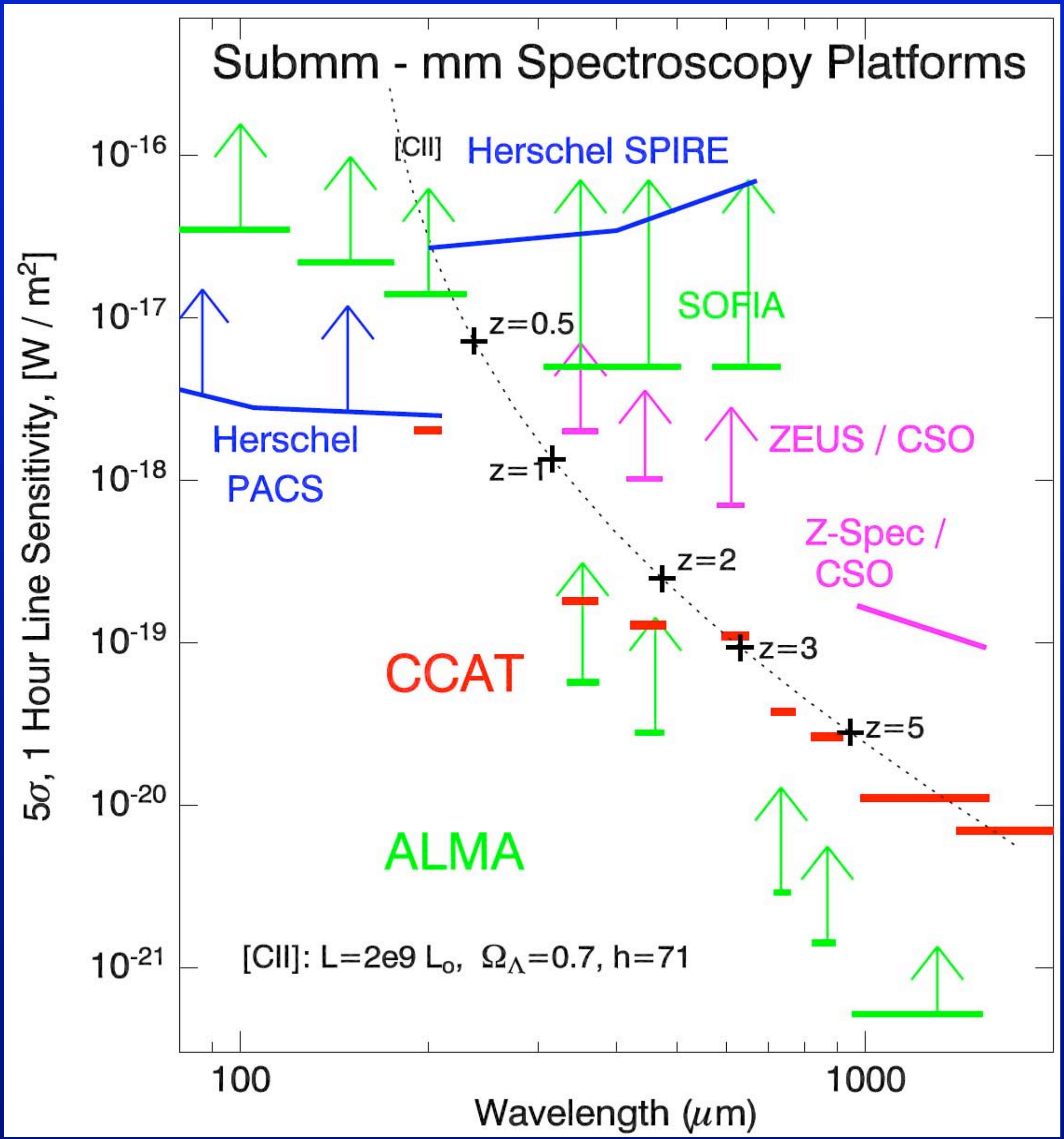

- Herschel, SOFIA -- small collecting area, no substantial advantage since warm apertures.
- CCAT less sensitive than ALMA, but with full window bandwidth, CCAT can carry out spectroscopic surveys on galaxies with comparable speed.
- Can be even faster if coupling many galaxies at once.

850 micron N(S) is to first order a luminosity function

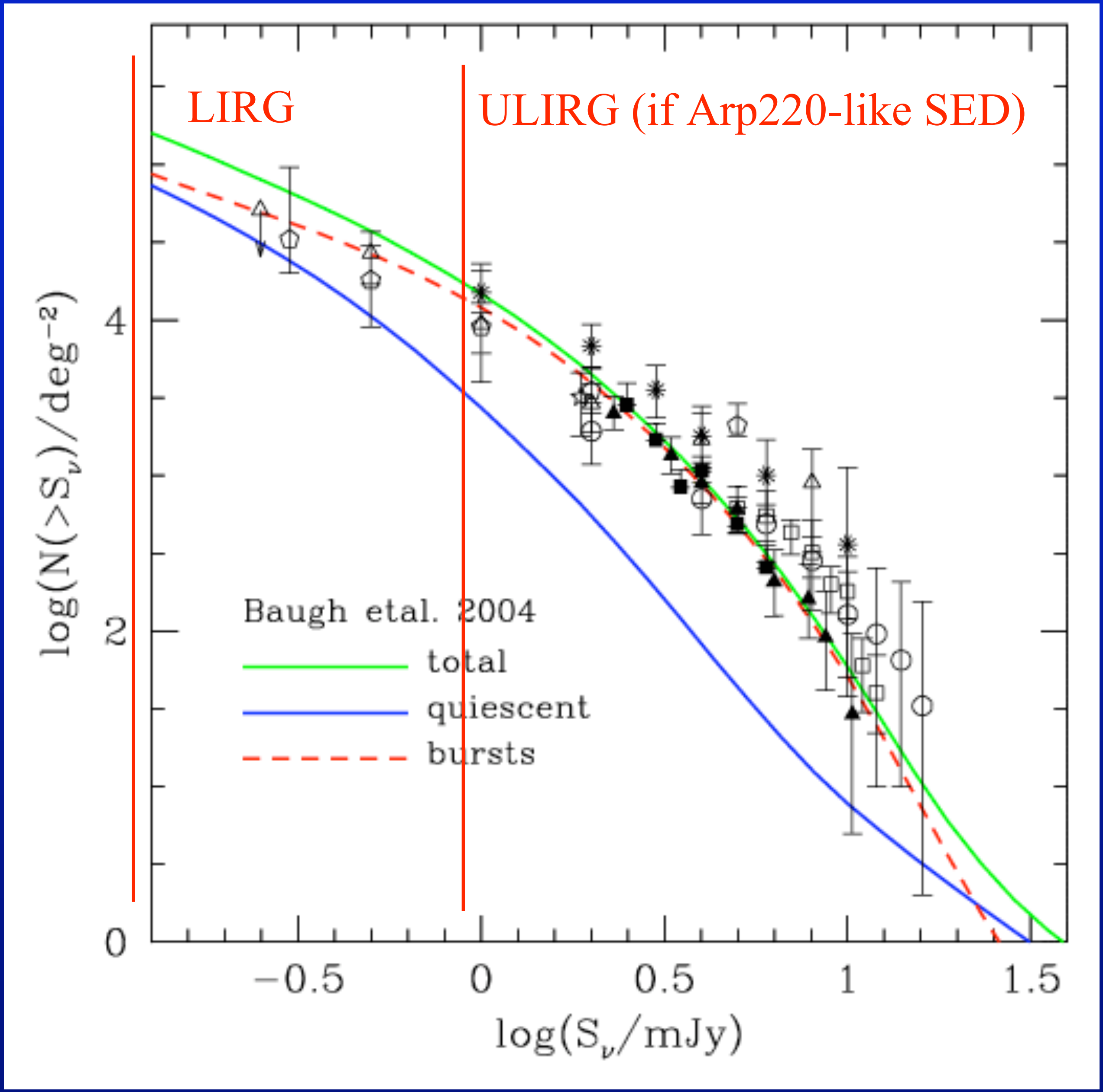

Models from A. Benson et al. (Galform group)

modified IMF and star formation timescale included to reproduce 850 micron counts

Models provide approach to CCAT population z distribution: Apply to C+

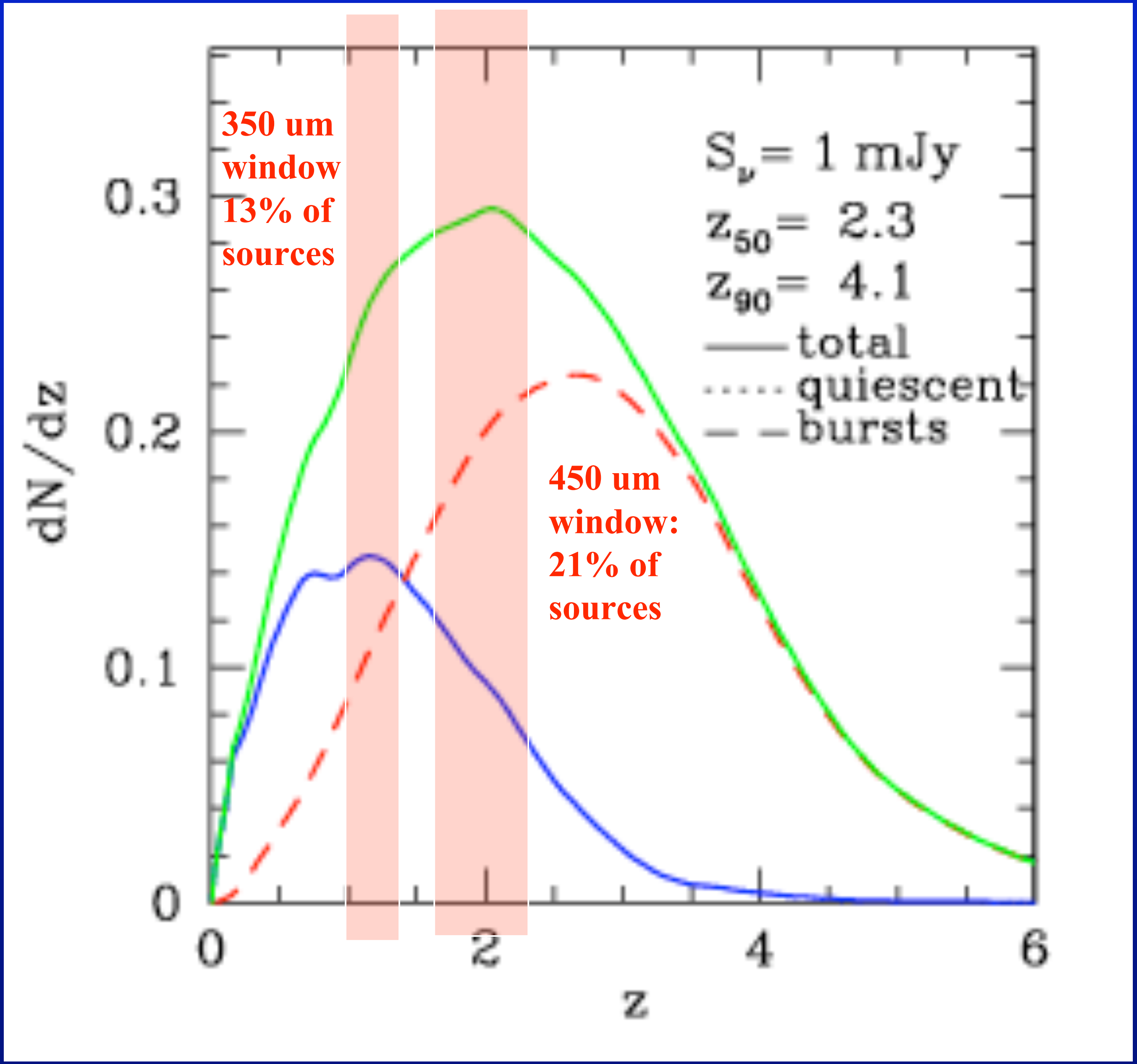

350 & 450 microns window are likely to access 31% of the 850 micron population in C+

Redshift Distribution from GALFORM model -- similar to Chapman

C+ Line luminosity fraction -> from Maiolano 05

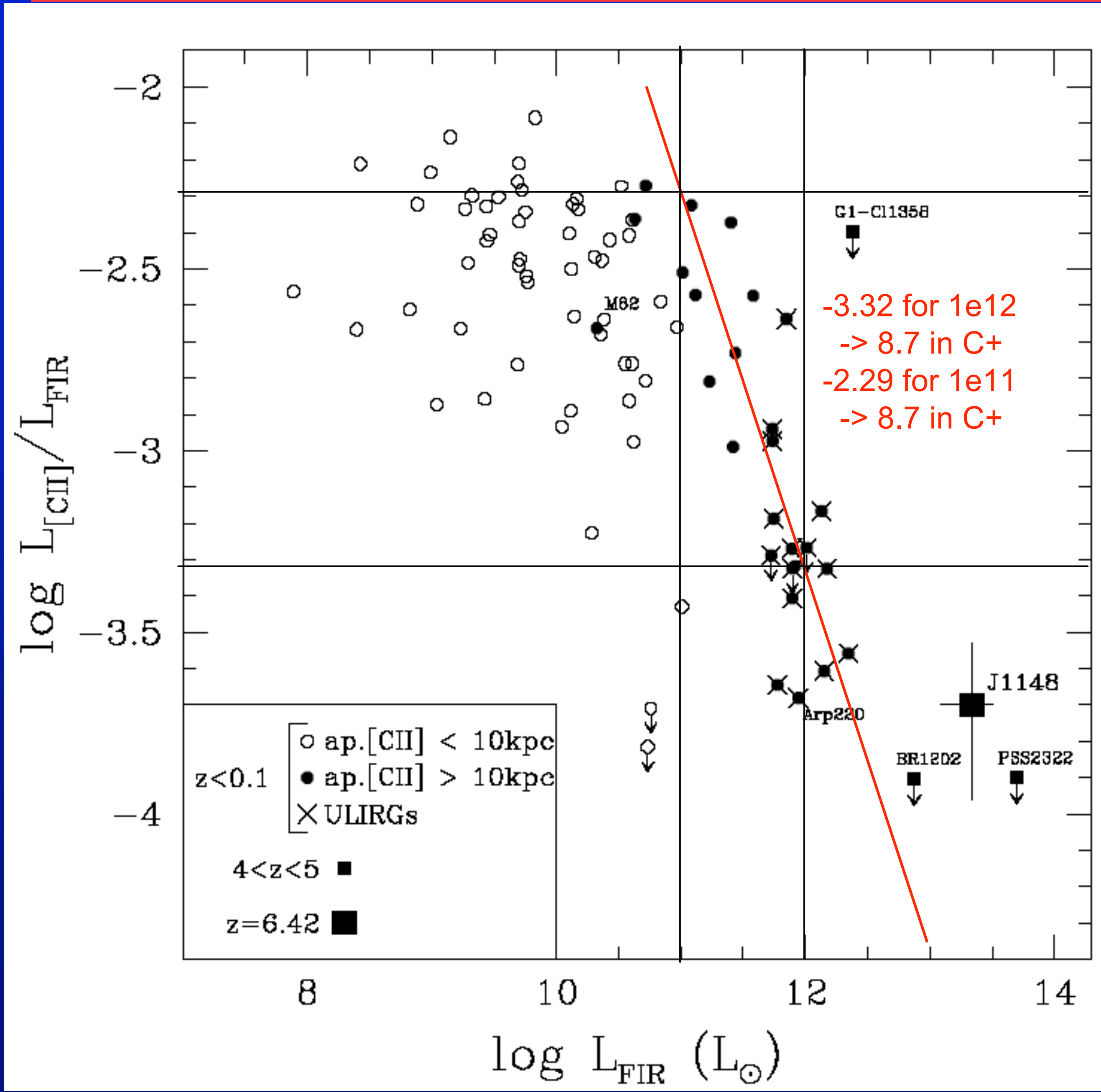

Local-universe LIRGS and ULIRGs have similar C+ intensities
-> Saturation of C+

Redshifted C+ Detectability with CCAT (JXZ)

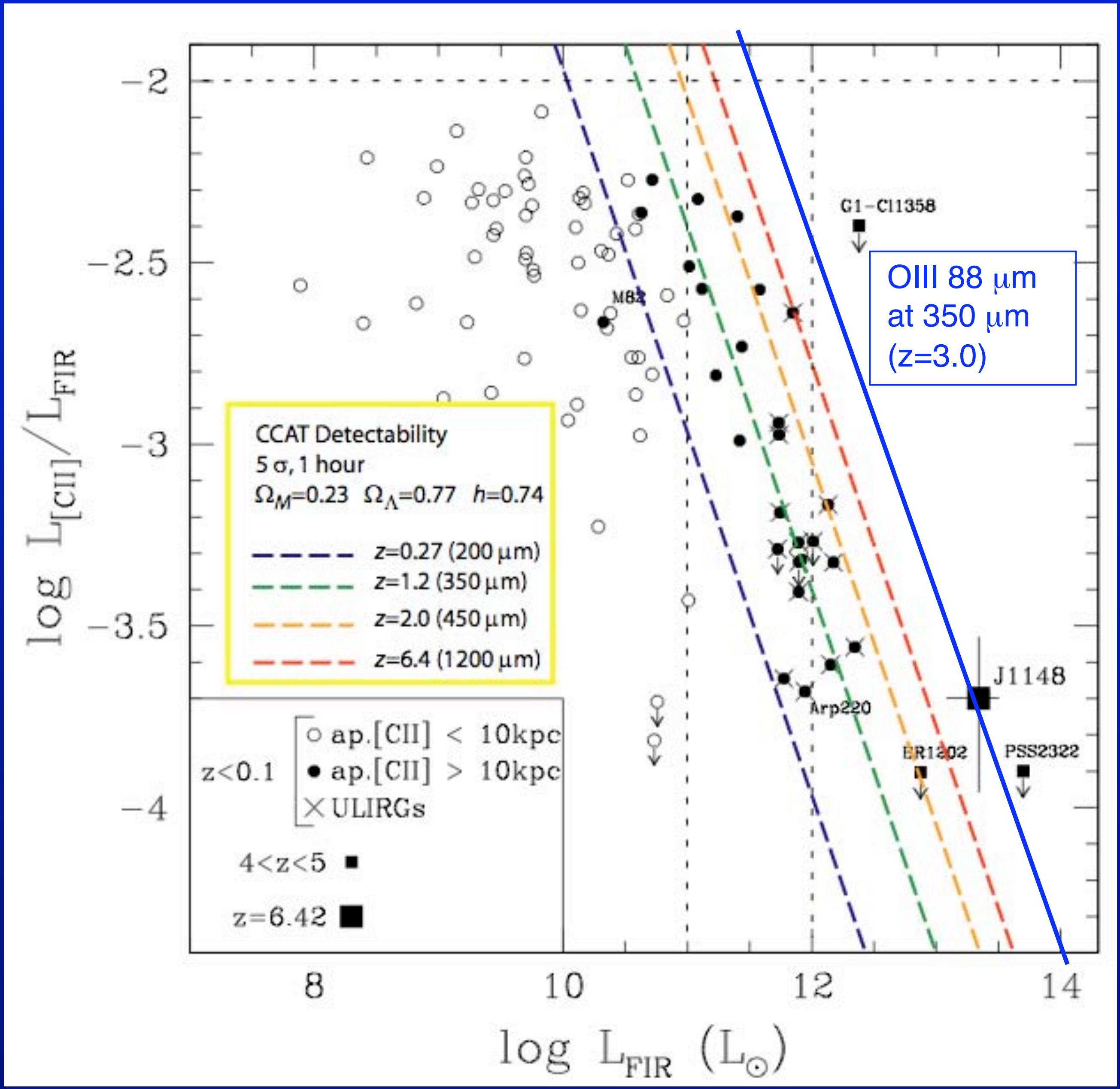

- *Constant C+ luminosity (log L_{C+}~8.7) for LIRGS to ULIRGS*
- *-> CCAT 350 μm sensitivities well-matched to these sources at redshift 1-1.4*
- *88 μm [OIII] detectable ULIRGS at z=3 if f_{line} > 0.003*

Redshifted C+ Detectability with CCAT

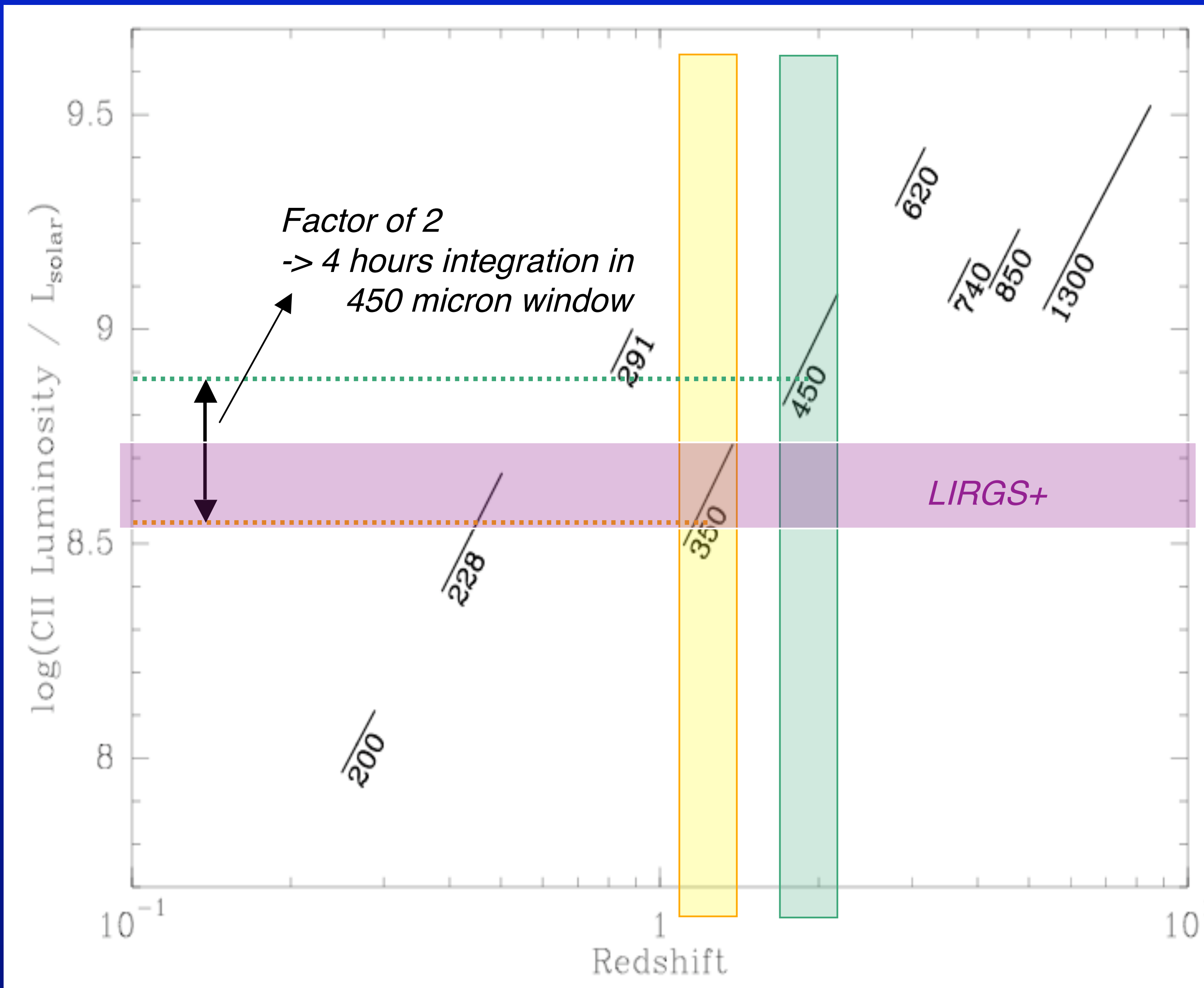

- Constant C+ luminosity (log L_{C+}~ 8.7) for LIRGS+
- -> CCAT 350 μm 1-hour sensitivity well-matched to these sources at redshift 1-1.4
- 4 hours @ 450 μm (z ~ 1.8-2.2) for the same sources.

How many such sources are there per area per redshift?

MIPS 24um sensitivity, redshift selection

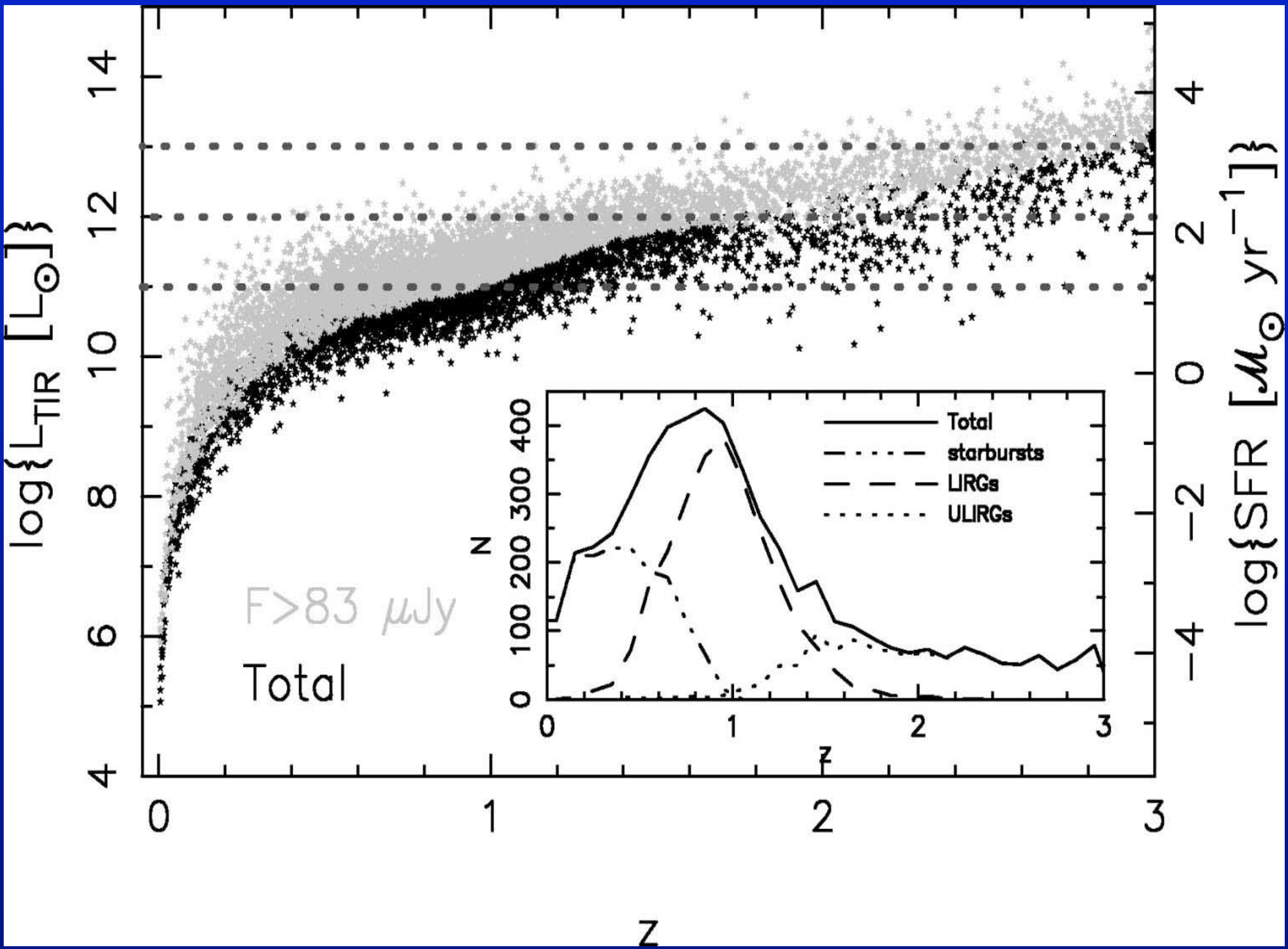

Perez-Gonzalez et al. (2006)

24 micron surveys (MIPS GTO team):

Spectroscopic and photometric redshifts

Use SED models to estimate luminosities from 24 micron fluxes

LIRGS to z~1, ULIRGS to z~2

Source populations for CCAT C+ spectroscopy

MIPS 24 mm surveys:

Use SED model and photometric redshifts to derive luminosity function at various redshifts (Papovich, Perez-Gonzalez, LeFloc'h, Egami, et al.)

MIPS 24 reaches out to z~1 for LIRGS, z~2 with ULIRGS

Egami, LeFloc'h et al measure ~1440 galaxies per square degree with log L > 11.25 at 1.0 < z < 1.2

According to a reasonable 850 micron redshift distribution based on e.g. Chapman et al. measurements (w/ recent z~1 additions) or Benson model, this redshift range should account for 5% of the total 850 micron sources at any given flux density.

This implies 3e4 total galaxies per sq deg with log L > 11.25 per sq deg ->
matched by 850 micron counts.

So we have a z~1 population measured at both 24 and 850.

- ***850 spans the redshift range with almost uniform selection, but shallow in L***
  - ***shows redshift range, extrapolate to lower- L***
- ***24 is biased toward low-z (z~1), but deep in L -- approaching knee at z~1 LIRG***

Source densities for C+ spectroscopy with CCAT

In the 350 micron window at redshift 1-1.2 (low-z half of the window),

Density of Log L > 1e11 sources = 7.1 e4 x 0.2 x 0.24 = 3.4 e3

= 36 galaxies per square degree per 300 km/s spectral bin

= 1 source per 40,000 CCAT beams per spectral bin

Extrapolating to the 450 micron window (redshift 1.8-2.0 is low-z half of the window) using a Chapman or Benson redhift distribution.

Density of Log L> 1e11 sources = 7.1e4 x 0.2 x 0.29 = 4.3 e3

= 62 galaxies per square degree per spectral bin

= 1 source per 14,000 CCAT beams per spectral bin

Options for CCAT spectrometers

- Grating spectrometer is the best choice for point sources.
  - 1^{st} order → octave of instantaneous bandwidth
    - Potential for 350, 450 micron windows simultaneously
  - Good efficiency
  - Only moderate resolution
  - Potential for multi-object capability further multiplies efficiency
- Fabry-Perot naturally accommodates spectral mapping at discrete (known) frequencies.
  - Offers potential for high-resolution (R~10,000) over modest fields
  - But scanning time results in sensitivity penalty, esp for searching
- Fourier transform spectrometer (FTS) couples the full band to a single detector.
  - Sensitivity penalty
- Heterodyne receivers provide the highest spectral resolution.
  - But suffer from quantum noise

    $NEP_{QN} \sim h\nu\,[\delta\nu]^{1/2}$ vs. $NEP_{\mathbf{BG}} \sim h\nu\,[n\,(n+1)\,\delta\nu]^{1/2}$
  - Also offer limited bandwidth:
    - 10 GHz IF bandwidth at 1 THz gives $\nu / \Delta\nu \sim 100$

CCAT Imaging Fabry-Perot Interferometer

SPIFI demonstrates concept at JCMT & the South Pole

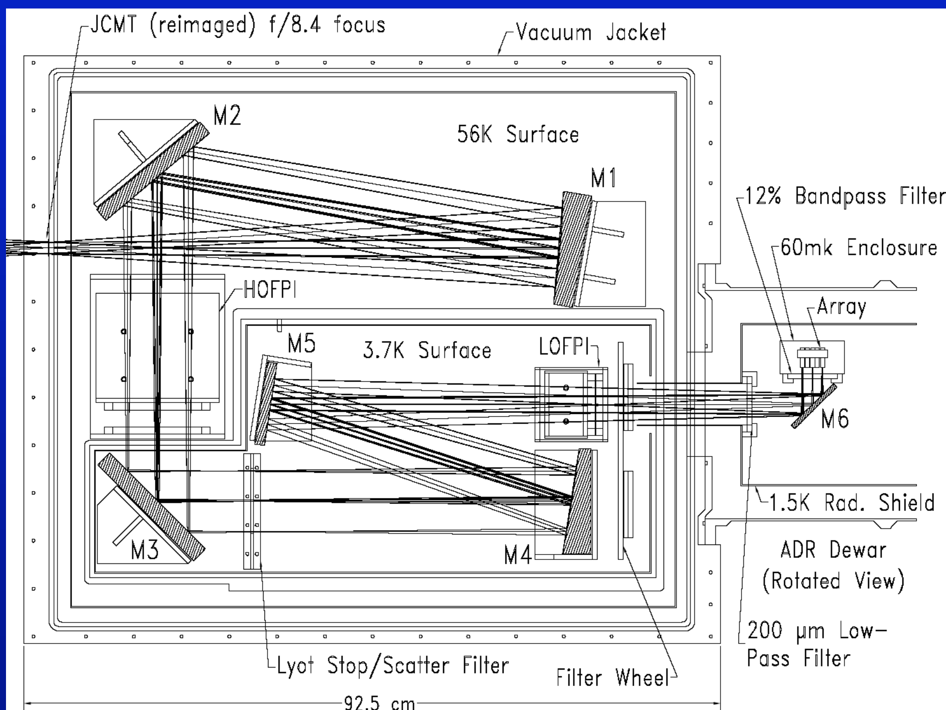

5x5 spatial array, two scanning FPs provide R up to 10,000 at 200-500 microns

60 mK ADR-cooled focal plane

Scope of CCAT Imaging Fabry-Perot

CCAT -IFPI will be much larger than SPIFI due to the large throughput
Limitation is beam divergence in the high-res FP.
$D_{col} \sim 1.5\ \lambda\ (R \times n_{beams})^{1/2}$ so $\Omega \sim D_{col}^{4} / (1.5\ \lambda\ R)^{2}$

	R=1000			R=10000		
wavelength	array	col. Bm.	sq deg	array	spacing	d locol
220.0	256	15.2	1.31E-02	44	18.33	2.23
330.0	196	20.0	1.73E-02	20	27.50	2.26
370.0	156	20.0	1.37E-02	16	30.83	2.27
430.0	116	20.1	1.03E-02	12	35.83	2.28
490.0	90	20.1	8.02E-03	8	40.83	2.12
650.0	51	20.1	4.53E-03	5	54.17	2.23
850.0	30	20.2	2.68E-03	3	70.83	2.25
1200.0	15	20.1	1.34E-03	1.5	100.00	2.25

11' x 11' field

Will require detailed optical design

Field size driven by 20 cm beam, assumes no spatial oversampling

1-D field size for 20 cm beam

High-order FP spacing (mm) w/ F=60

Order-sorter also requires collimated 2.2cm (or slow) beam

CCAT IFPI will be much larger than SPIFI due to the huge throughput

8 x 20 cm = 160 cm collimator focus

Full field at f/8: 20 cm window!

Etalon spacing is modest: few cm even for 650 μm

Collimated beam + overheads: 25 cm dia (and etalon must be near pupil)

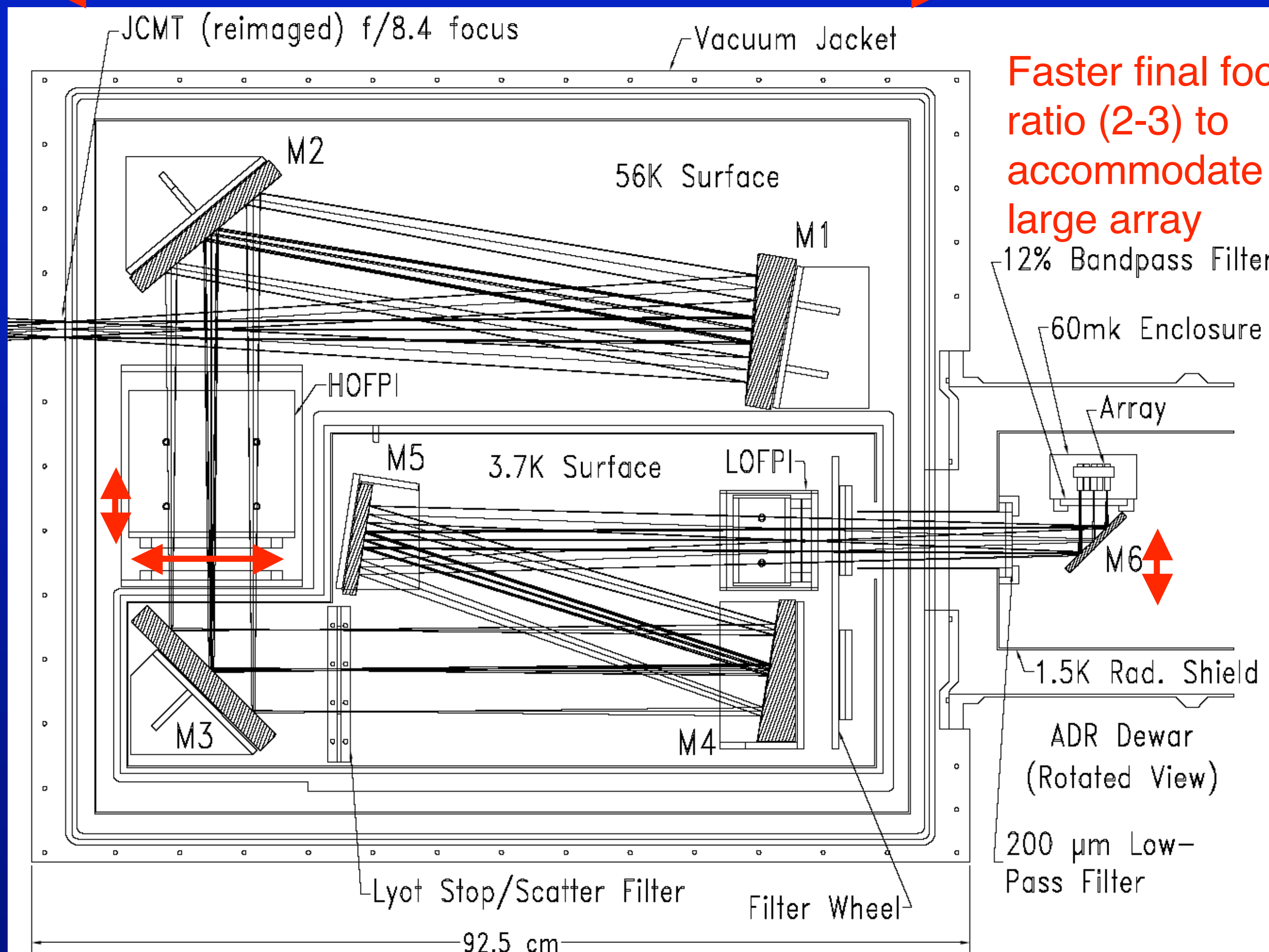

Faster final focal ratio (2-3) to accommodate large array

Array is as large as 10 cm

Factor of two in all dimensions of the optical train

C+ Detection Rate: Comparison Between FP & Grating

Could a Fabry-Perot serve to select sources at specific redshift from a field ?

Fabry-Perot

Source detection rate =

$dN / dz \times \Omega$

dN / dz = 36 -- 62 per square deg, per res el.

= 1.7e-2 sq deg

Rate = 0.6-0.7

Grating

Source detection rate =

z_fraction x N_mos

z_fraction = 0.3 (including 350 and 450)

N_mos = ? (10-100)

Rate = 0.3 x 10-100

~FEW SOURCES PER HOUR

Most optimistic R=1000 FP at 350 microns: 200 x 200 = 4e4 beams or 1.7e-2 sq deg

Take 10 resolution element scan: Gives 1.7e-2 x 36 x 10 = 6 LIRG+ sources
In 10 hours observation. Doesn't look good, not enough volume due to finite z

Yes, but source densities are low enough that detection rate in the field will be low.
Broadband grating is faster if you can get a couple even a couple sources

Examples of submillimeter-wave echelle grating: ZEUS for the JCMT / APEX

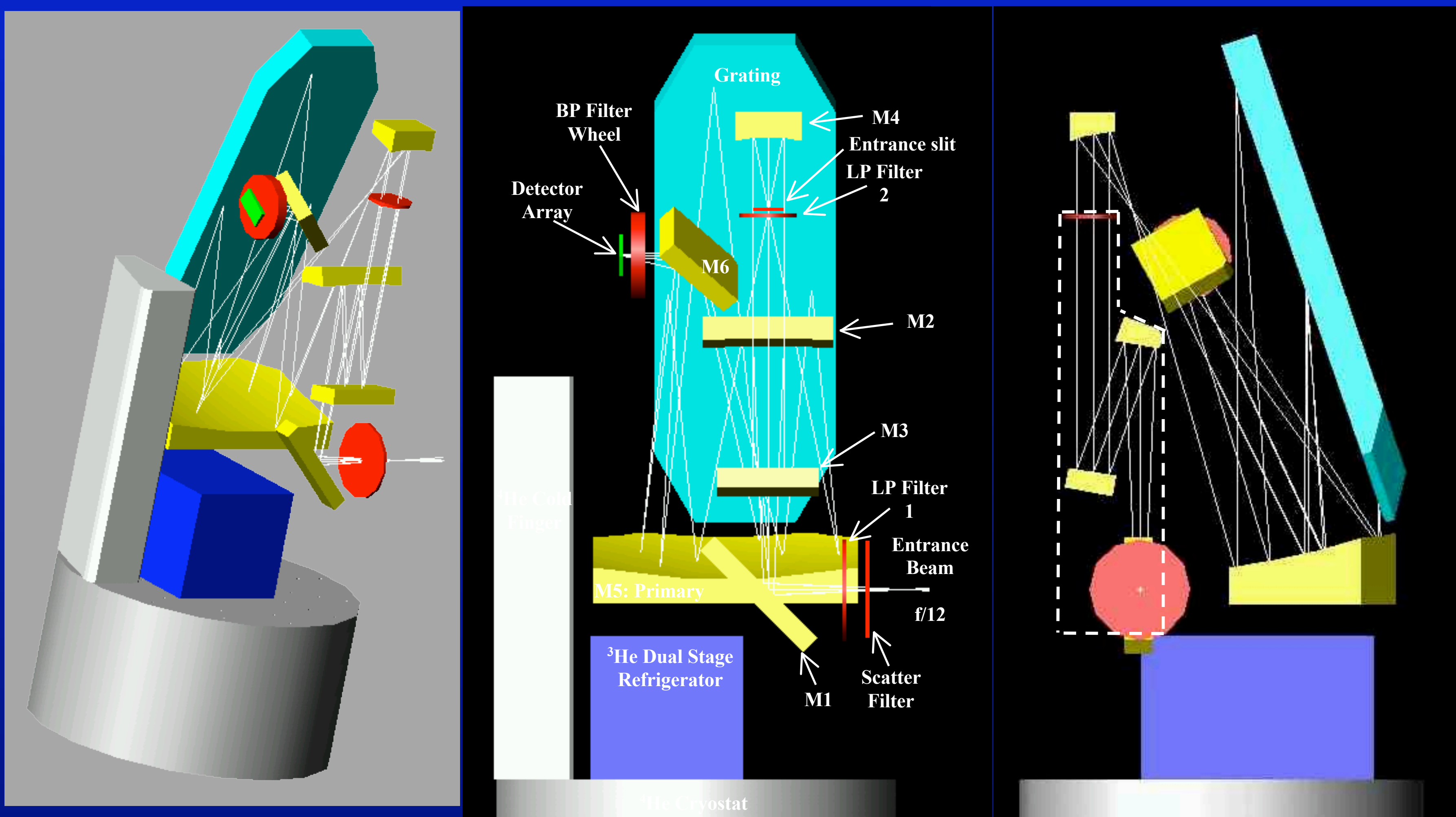

Cornell -- Stacey, Haley-Dunsheath, Nikola

350, 450 μm windows w/ R~1000-1500

ZEUS Grating

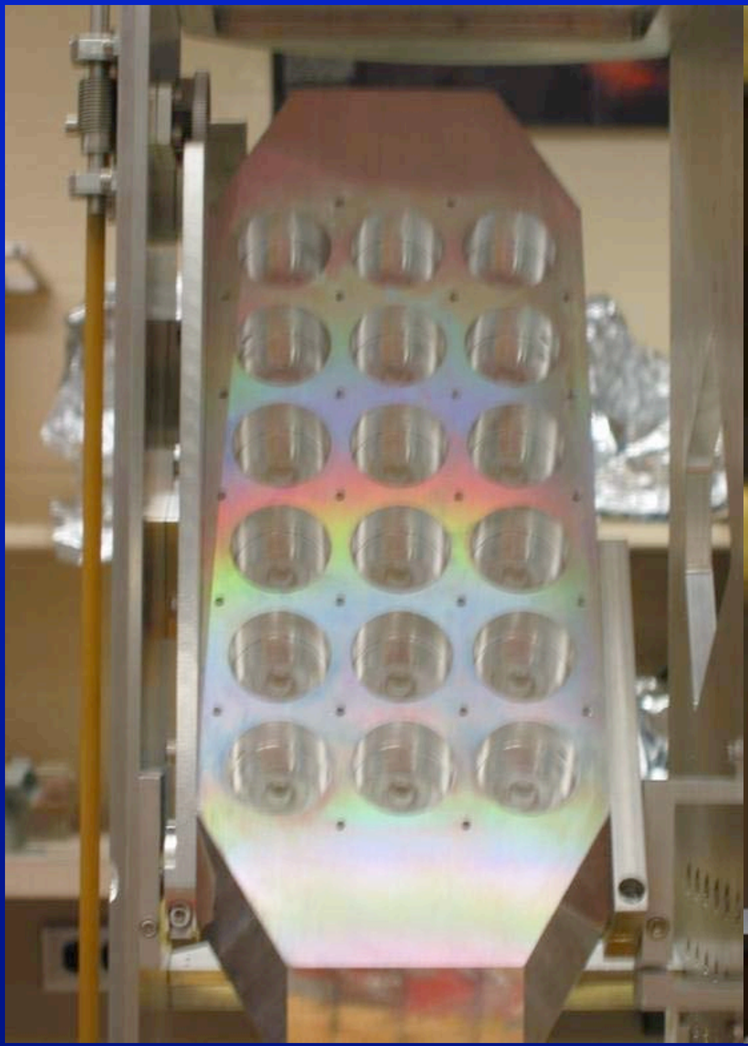

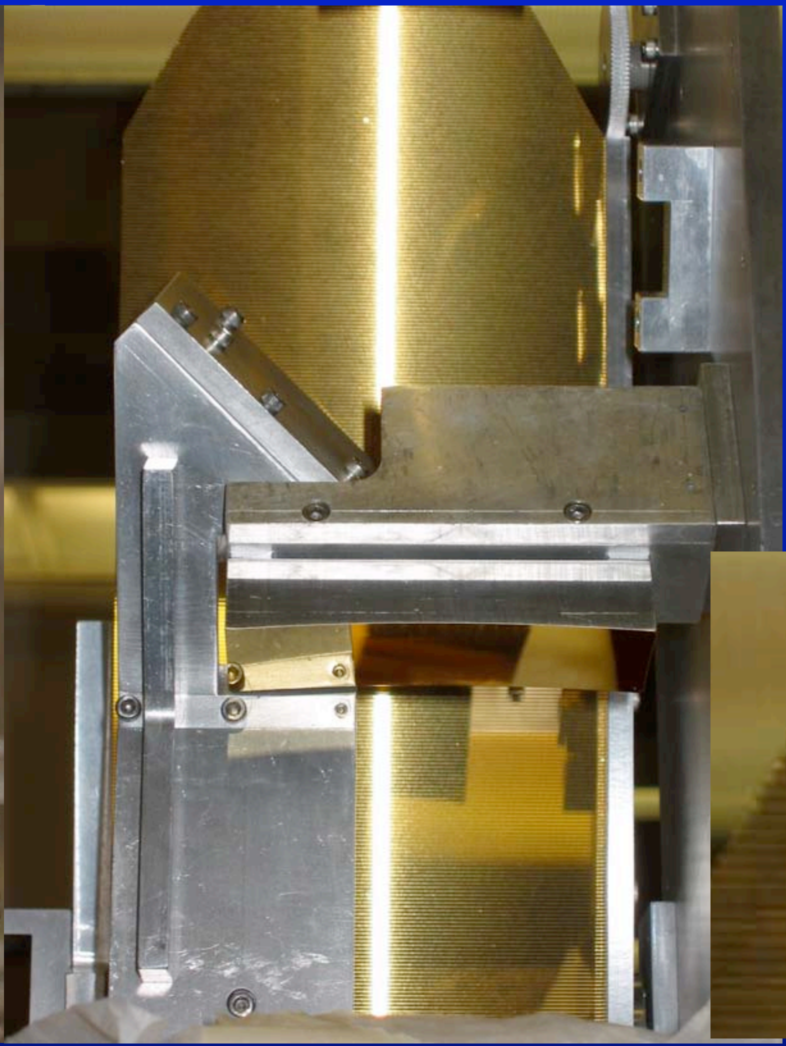

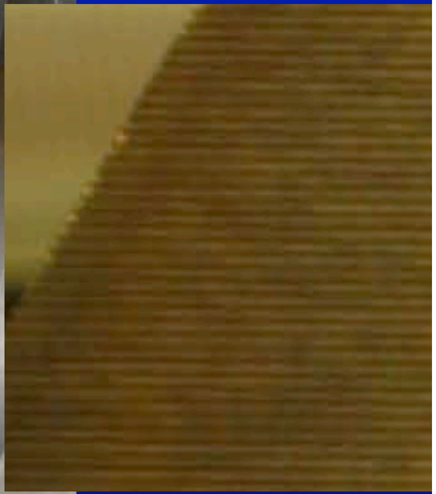

- *Manufactured by Zumtobel Staff GmbH (Austria).*

A new R~1000 echelle spectrometer for CCAT

Design: Grating 816 micron pitch

Tilt	λ min	λ max	BW	R	slit	# pix on slit
3rd order						
58 deg	439	485	9.7%	800		
54 deg	418	462	9.3%	822	5.8	2.08
62 deg	456	504	11.0%	903		
4th order						
57 deg	330	356	7.1%	1100	4.3	1.44
63 deg	350	377	8.2%	1245		
6th order						
56.5 deg	221.3	232.7	5.0%	1646	2.7	0.96
7th order						
60.5 deg	198.7	207.4	4.3%	1920	2.7	0.96

Assuming 128 spectral element array

-- e.g. 0.86 mm pixels -- f/2.5 spectrometer, slightly oversampled

Angular deviation off the grating 18 deg total.

collimator must be oversized by 12 cm !

--> 30 cm diameter collimator

--> grating 30 cm by 40 cm, to accommodate spatial throughput

CCAT echelle will be large

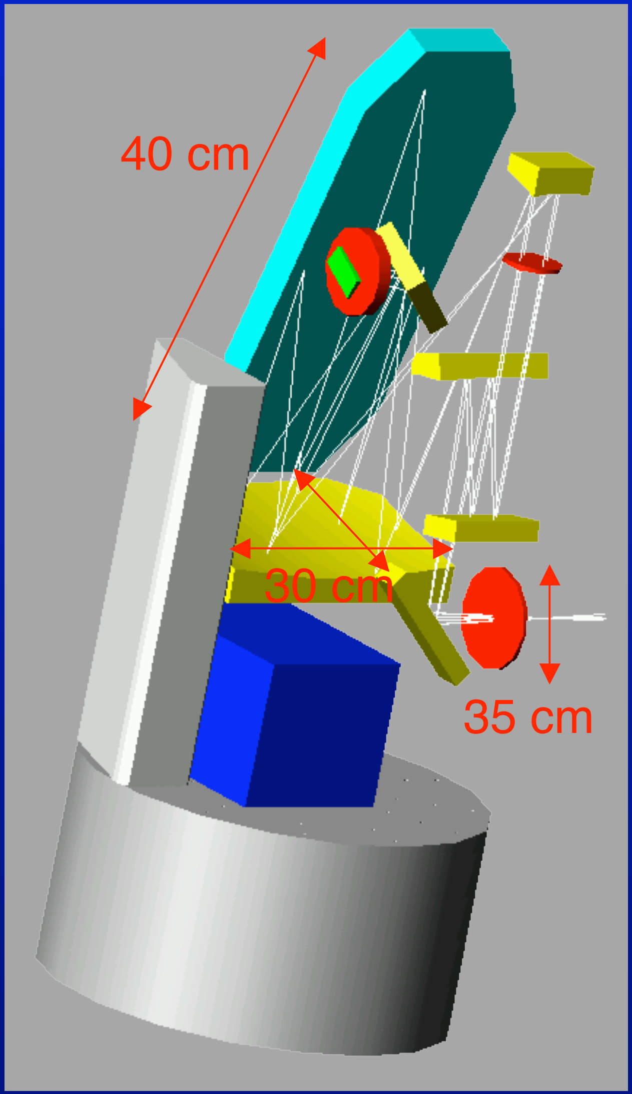

So grating and collimator are a large fraction of 1 meter in all dimensions -- 1.5-2 times larger than ZEUS

Reimaging optics size will depend on the size of the slit, but also grows relative to ZEUS:
--scales as telescope f# x #of beams: Relative to ZEUS, CCAT echelle will have 8/12 x 128/32 = 2.7 times larger reimaging optics.

- **Requires 35 cm (+ overhead) window if reimaged from telescope focus inside cryostat (but can be shaped like a slit)**

Optics envelope inside cryostat approaching 1 meter in all dimensions.

Large but doable.

True broadband spectroscopy in the submillimeter:
Z-Spec, a 1st order grating covering 190-305 GHz.

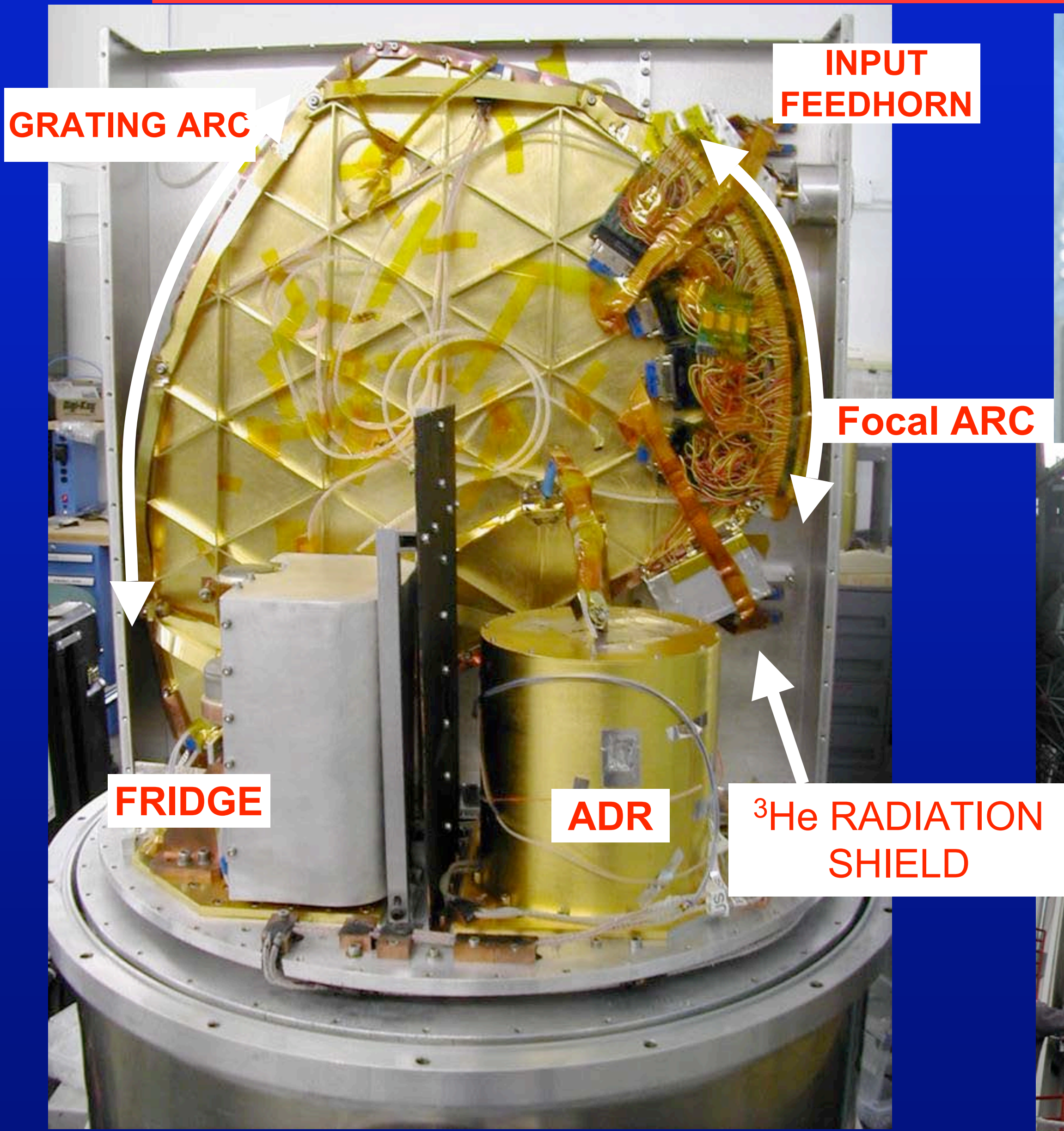

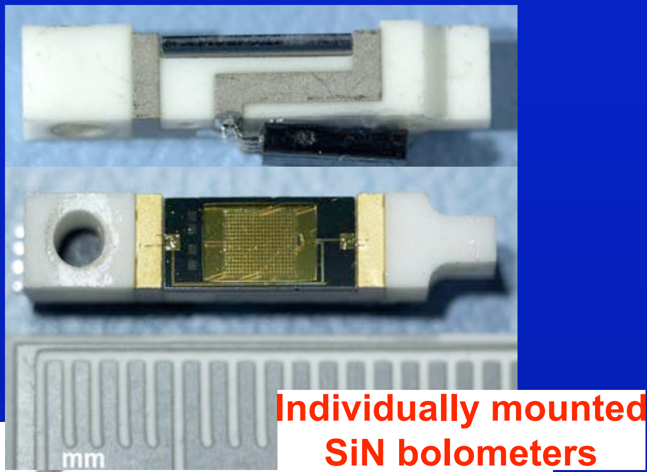

True Broadband Spectroscopy in the Submillimeter: Z-Spec, a 1st order grating covering 190-305 GHz

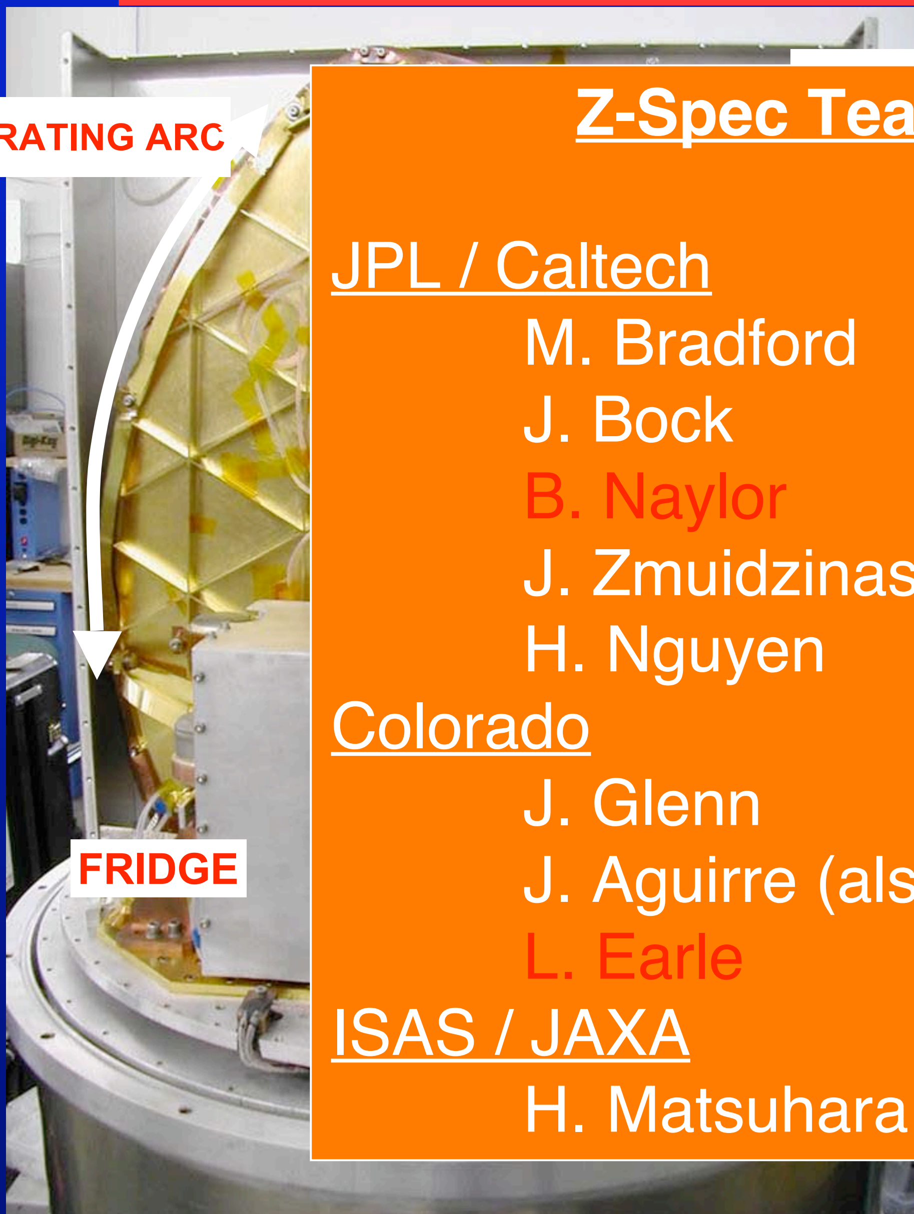

Z-Spec Team

JPL / Caltech
- M. Bradford
- J. Bock
- B. Naylor
- J. Zmuidzinas
- H. Nguyen

Colorado
- J. Glenn
- J. Aguirre (also NRAO)
- L. Earle

ISAS / JAXA
- H. Matsuhara

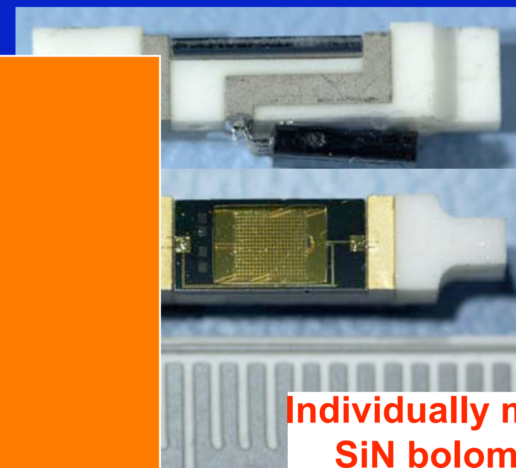

Z-Spec approaching its photon-noise limits at the CSO

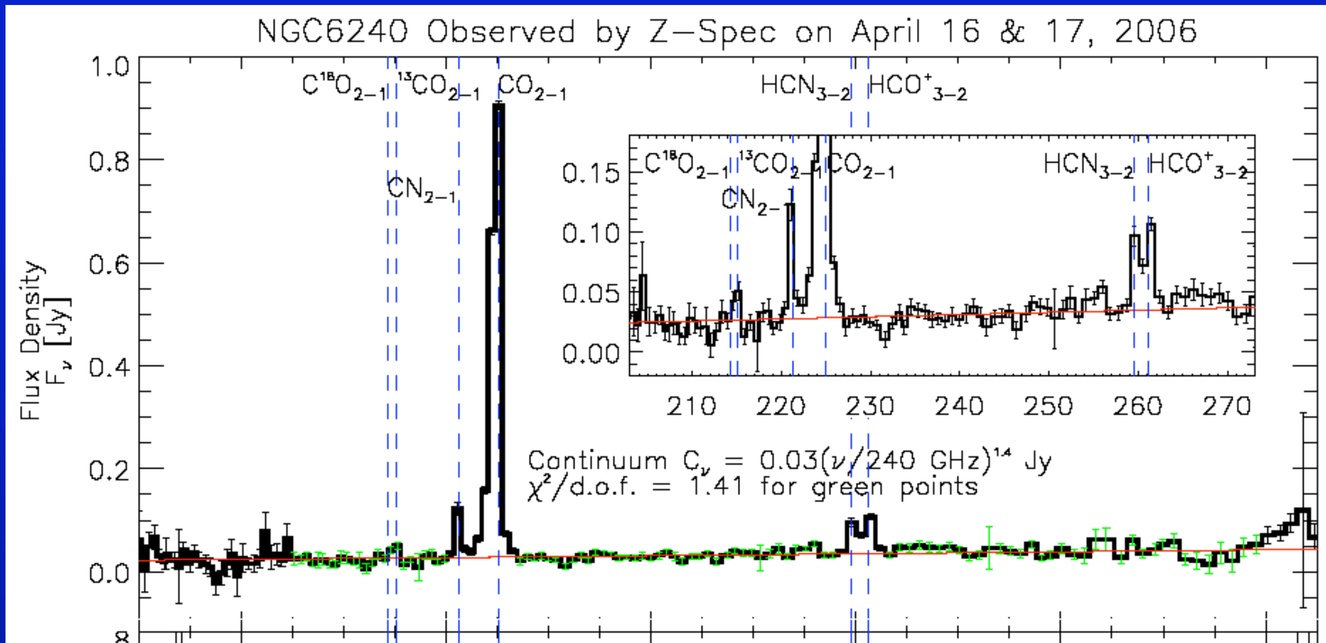

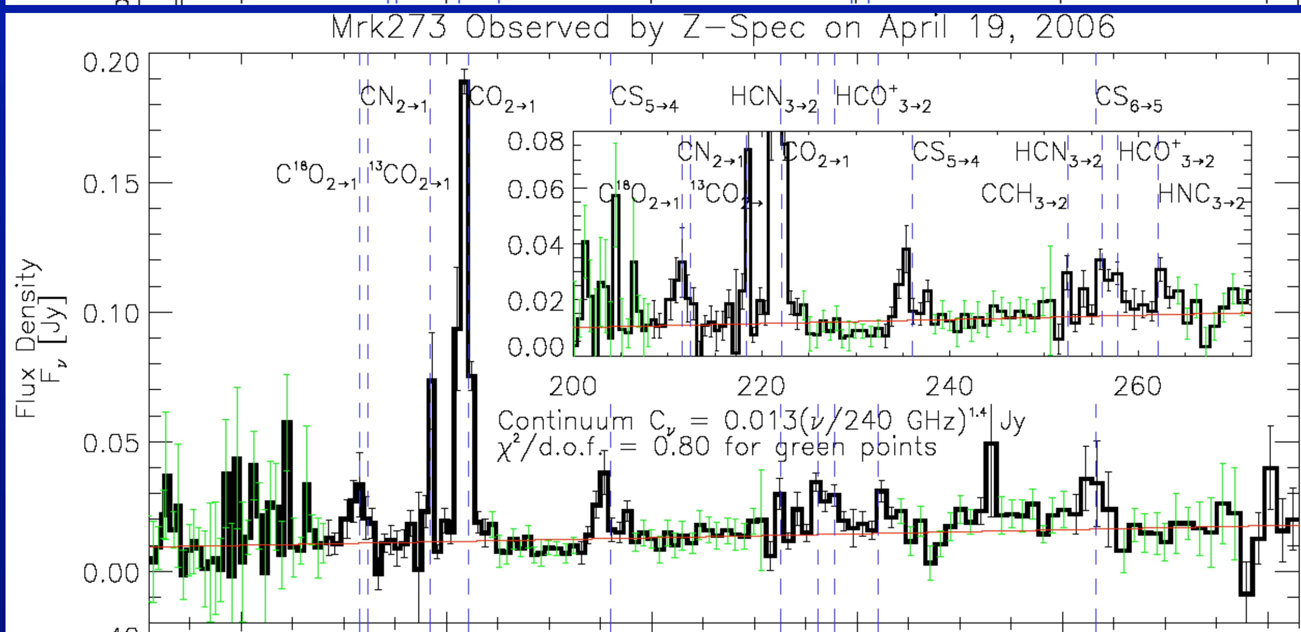

200 GHz

300 GHz

ULIRG spectroscopy for CO, isotopes, density tracers.

Bret Naylor Ph.D. dissertation

High-redshift observations coming this winter.

A similar device could cover the entire 350 and 450 μm windows simultaneously at R~800

Both waveguide and free-space echelle grating spectrometers could accommodate a mulit-object front end.

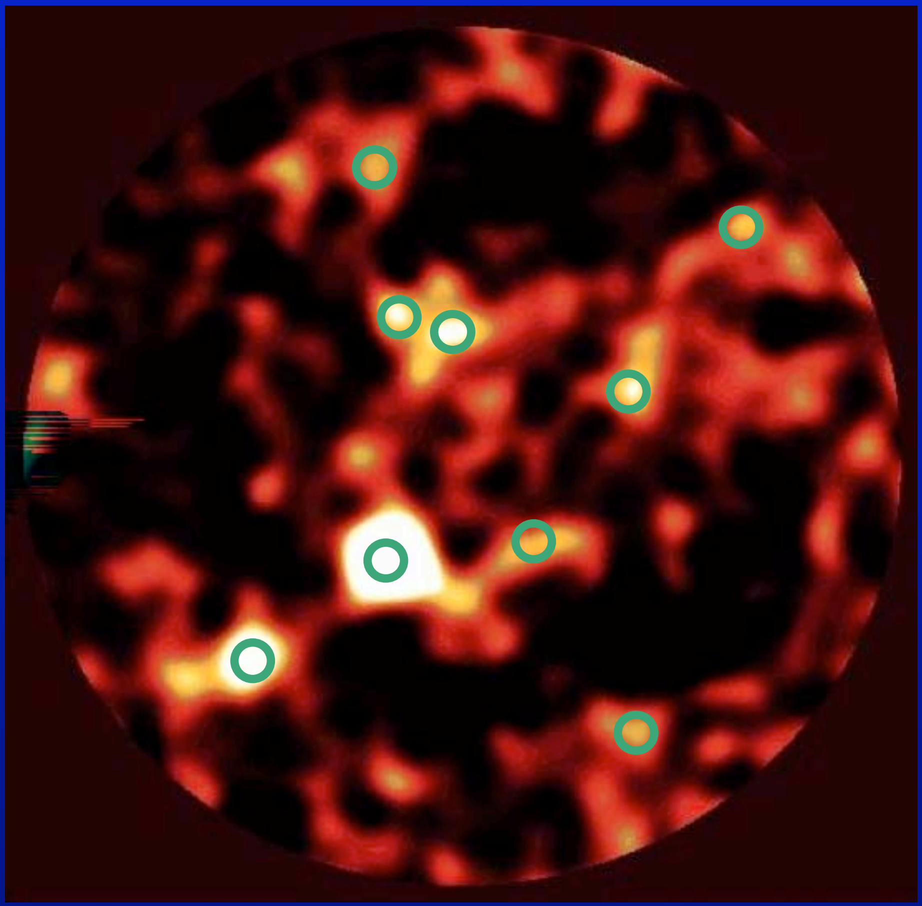

Hughes et al. SCUBA HDF North

- Remember CCAT continuum surveys at 350, 450 will go much deeper
- Will be ~110 LIRG+ galaxies in this 5.6 sq arcmin field.

Source density of LIRG+ galaxies:
71,000 per square degree
= 1 every 180 sq arcsec
= 1 every 10 CCAT 350 / 450 mm beams.

With slit of 1 x 30 beams:
Could position slit to get at least 2, perhaps 3 sources with no additional effort except field rotation.

Ideal system:

- 10-50 feeds patrolling 4 sq arcmin field.
- 8 x 8 cm in the native f/8 telescope focus.
- feeding slit of echelle or multiple Z-Spec-like devices
- Mirror arms or flexible waveguide

Flexible Dielectric Waveguide -- 200 μm polyethlyene monofilament

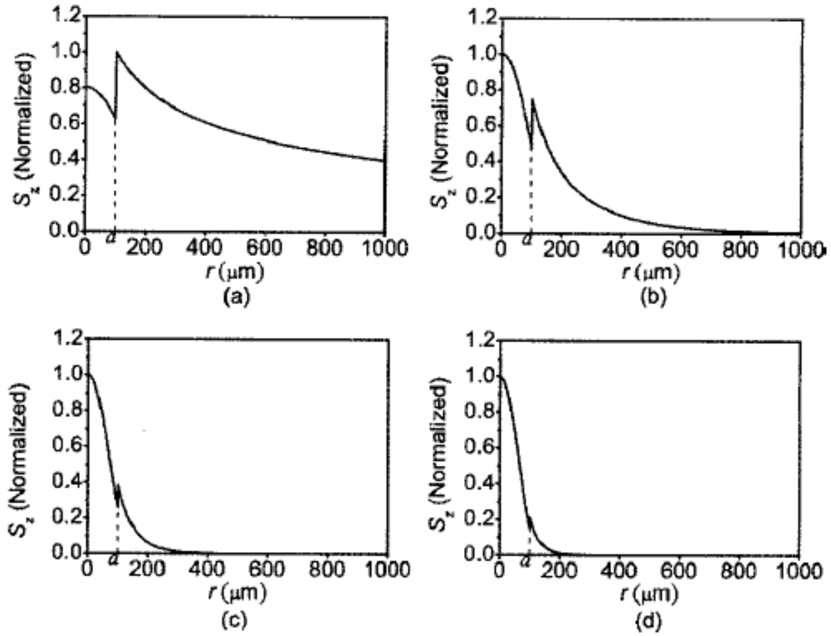

Fig. 1. Spatial distribution of the z-direction Poynting vector about a 200 μm diameter ($a=100$ μm) PE wire at frequencies of (a) 300, (b) 500, (c) 700, and (d) 900 GHz. The PE wire is assumed to be surrounded with air.

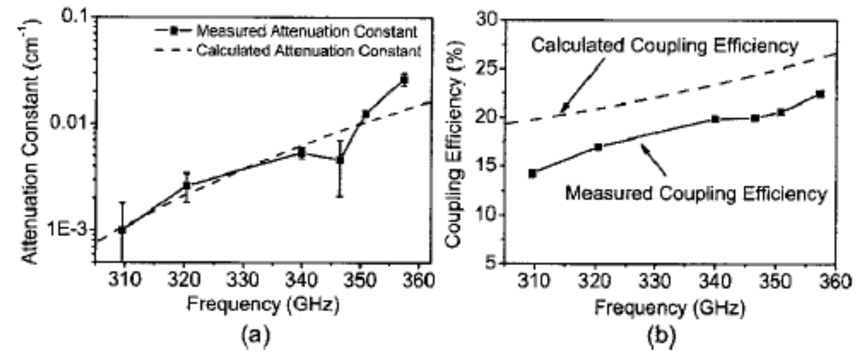

Fig. 2. (a) Measured fiber attenuation constant of the 200 μm diameter PE wire in the frequency range 310–360 GHz. For comparison, the calculated fiber attenuation constant of an ideal THz fiber, whose absorption constant α is assumed to be 1 cm^{-1} in this frequency range, is shown. (b) Comparison of measured and calculated coupling efficiency of the PE wire in the frequency range 310–360 GHz.

Chen et al. 2006

$$\alpha_f = \left| \frac{1}{P}\frac{\mathrm{d}P}{\mathrm{d}z} \right| = \frac{\sigma \int |E|^2 \mathrm{d}\tau}{\left| \int S_z \mathrm{d}\tau \right|},$$

Tradeoff between guiding and loss
less field inside -- lower loss but
cannot bend sharply.
NEED BENDING MEASUREMENTS

Flexible low-loss waveguide -- concentrating the field energy into air

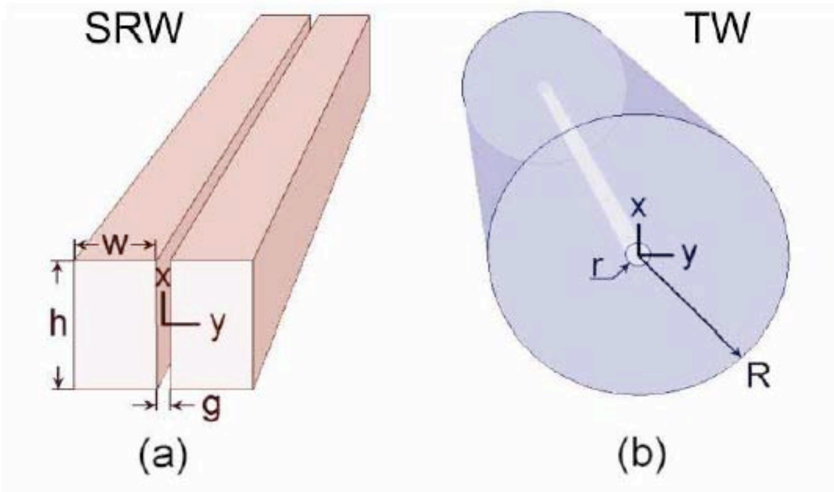

Fig. 1. Geometries of the considered dielectric waveguide structures: (a) A split rectangular waveguide and (b) a tube waveguide.

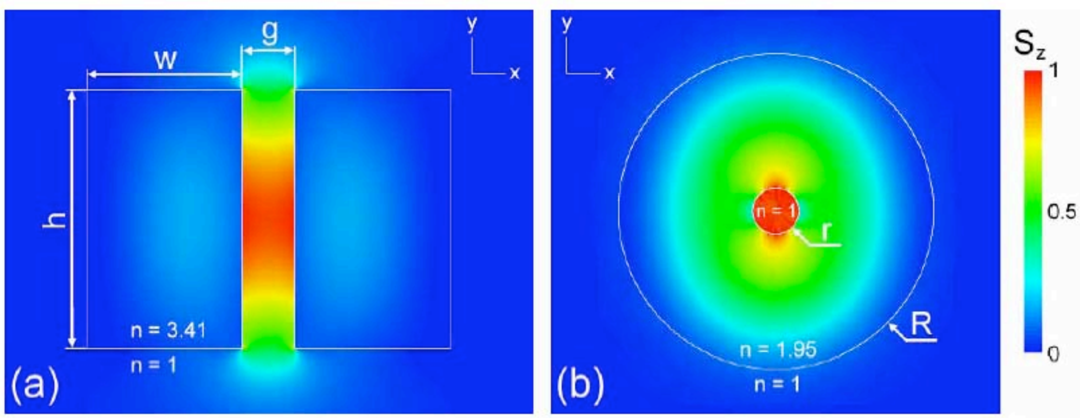

Fig. 2. Distribution of the normalized scalar z-component of the time-averaged Poynting vector S_z over a linear color scale in the cross section area of the waveguides. (a) Float-zone silicon split rectangular waveguide at $f = 0.7$ THz with $w = 54$ μm, $h = 90$ μm and $g = 18$ μm. (b) Fused silica tube waveguide at $f = 0.5$ THz with $R = 181.5$ μm and $r = 27$ μm.

$$\alpha_f = \left| \frac{1}{P}\frac{\mathrm{d}P}{\mathrm{d}z} \right| = \frac{\sigma \int |E|^2 \mathrm{d}\tau}{\left| \int S_z \mathrm{d}\tau \right|},$$

Nagel et al:
Split rectangular waveguide offers compromise of low loss, good confinement. But no measurements yet.

Flexible Dielectric Waveguides

Specifications

- Number – minimum of ten 10-cm seems quite feasible
- Bend radius of few cm seems feasible
- Acceptable loss – push toward short λs, waveguide loss not dominant: $T_{sky}(\tau350\mu m=0.25)$ = 70 K, T_{tel} = 20 K, T_{guide}(trans=60%) = 95 K
- *PTFE remains flexible at low temperatures!*

Manufacture

- Vendors – Zeus, custom extrusion houses
- Standard sizes – down to 710 μm
- Custom fabrication cost -- $1,200 per run of 2500 ft (underestimate?) – *fishing anyone?*

CU Seed Grant Proposal (Submitted yesterday)

- Funds -- $50k, 1 yr
- Collaboration: CU APS, EE, NIST, Colo. School of Mines
- Test setup: room temp diode detector; network analyzer – 400 GHz, *900 GHz*; cryo with TESs 850 μm; differential vs. metal
- Test variables: HDPE vs. PTFE; 350 & 850 μm; room temp, cryogenic loss; loss vs. bend radius; loss after many bends
- Simulations

J. Glenn

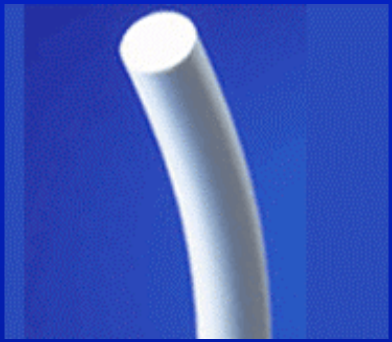

Zeus, Inc.

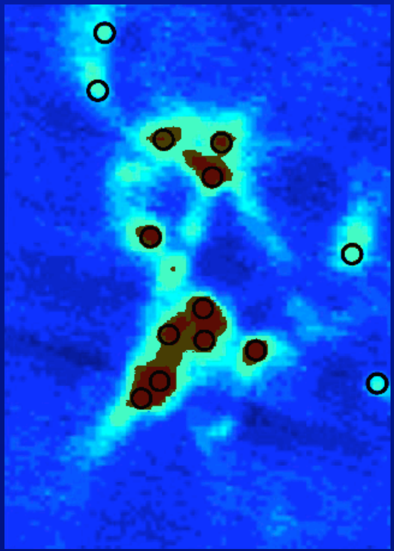

Ex. NGC1333

Detectors for CCAT spectroscopy --
TES or MKID technology being developed for flight

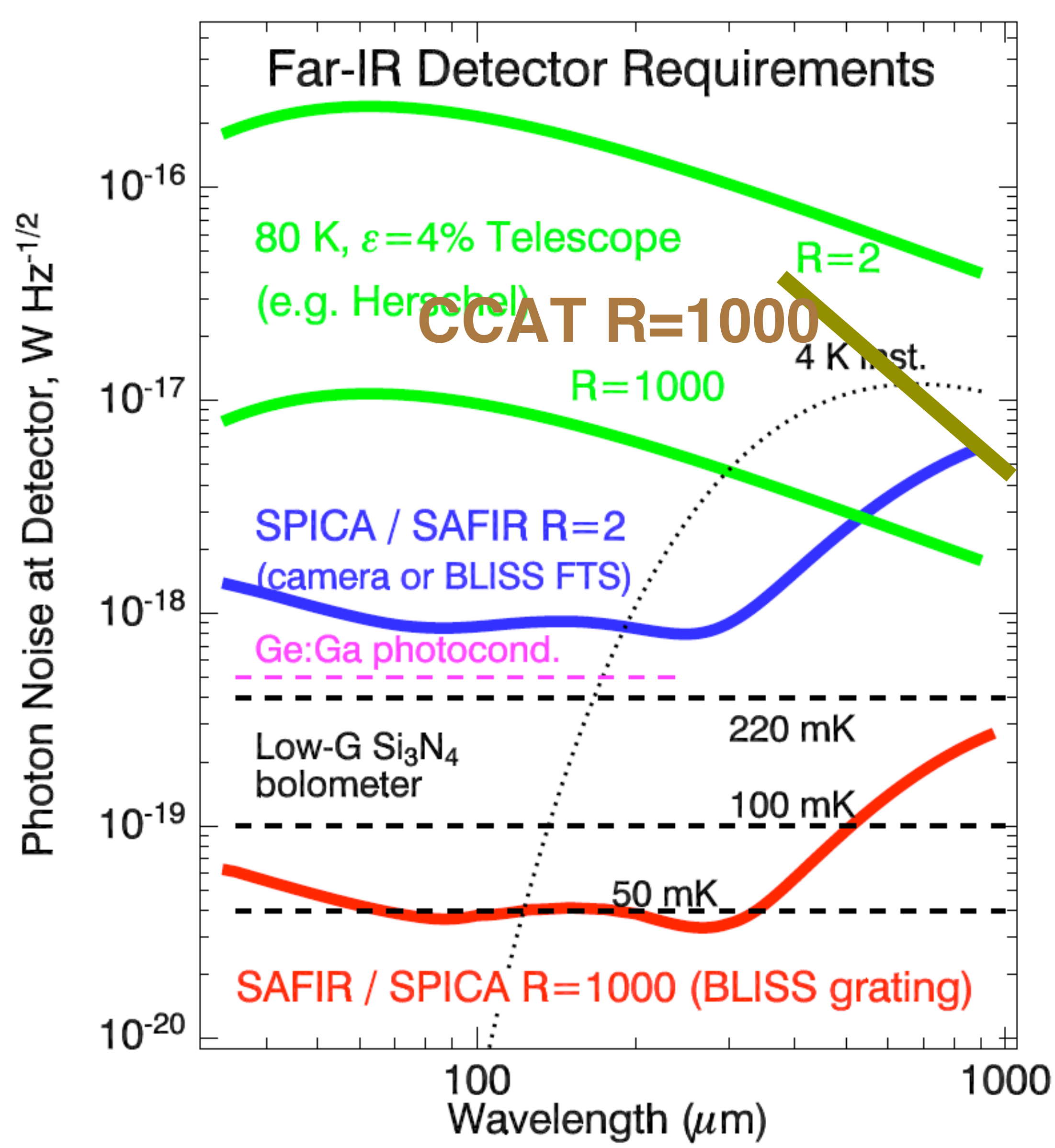

Want ~30 kpixel array for CCAT spectrometers.

Sensitive detectors are under development for low-background flight experiments.

Requirements for R=1000 at λ< 1 mm with the CCAT are of order 10^{-17} W $Hz^{-1/2}$.

Achievable with existing devices.

TES MUX can work equally well at these NEPs -- development is similar to that of SW CAM, SCUBA-2.

R~10,000 at the long wavelengths starts to become a relevant testbed for SAFIR / SPICA detectors.

4 K instrument: AΩ = 3 mm^2, Δλ/λ = 50 %, ε = 10 %

CCAT Spectrometer Telescope Requirements

- Very similar to cameras:
  - 1-2 tons of cryostat + electronics
  - 5-10 kW of electrical power
  - More modest field sizes -- few square arcmin
  - Similar data rates.
- BUT GRATING SPECTROMETER WOULD LIKE A CHOPPING SECONDARY
- Slit spectrometer needs field or instrument rotation capability
  - MOSSCCAT may be able to track sources (but not chop!)

CCAT Spectrometer Budget

- Option 1: Use modestly-upgraded Z-Spec and ZEUS
  - Labor: 10 FTE = $1.5 M,
  - Dual Z-Spec grating + detectors + electronics (NTD): $0.5 M
  - ADR + array for for ZEUS: $0.5 M
  - Total: $2.5 M for upgraded Z-Spec & ZEUS.
- Option 2: Dedicated Multi-Object CCAT Spectrometer
  - 30 kpix TES array + MUX + electronics: $6.7 M (NIST -- estimate from SW CAM camera)
  - Labor: 27 FTE: $4 M, includes spectrometer optics fabrication
  - Cryostat, pulse tube, ADR or dilution fridge: $0.5 M
  - Multi-object front end development + fabrication: $2.0 M
  - Total: $13.2 M

Conclusions

- Tens of thousands to millions of galaxies will be discovered in far-IR to millimeter continuum surveys in the next 15 years.
- Spectroscopic follow-up will be the bottleneck.
- CCAT can be competitive with ALMA for spectral surveying in the short submillimeter.
  - a multi-object broadband grating can exceed ALMA for spectral-survey follow-up of LIRG+ galaxies.
- Galaxies w/ $L > 10^{11}$ have ~constant C+ flux and are detectable with CCAT spectrograph.
  - ~1 hour in the 350 micron band
  - ~4 hours in the 450 micron band
  - together these bands will capture ~30% of all the 850 μm-selected sources
- Existing spectrographs with modest upgrades can reach close to the fundamental photon-noise limits of CCAT, but limited
- Ideal CCAT spectrometer is a multi-object low-order grating.
  - We CAN get redshifts: few to couple tens per hour.

Flexible Dielectric Waveguides

Previous Work

J. Glenn

- **System advantages:** simple, compact, elegant
- **Challenges:** absorption, high-frequency fabrication

Options

1. Powder-filled circular waveguides

- Tested at 10 (X-band) & *94 GHz (W-band)*
- PTFE cladding, 21-23 AWG (150 µm walls)
- Trans-Tech MCT-40 magnesium-calcium titanate, D-30 nickel-aluminum titanate, D-8512 barium titanate cores; grains ≤ 43 µm
- D-30 loss best: 25% over 10 cm
- Tapers/coupling characterized
- Unmeasurably small loss induced by bend radii < 4 cm

2. Monofilament – Best choice

•HDPE waveguide tested up to 300 GHz
•Rectangular: 560 µm x 280 µm
•Loss 19% over 10 cm; extrapolated to 35% @ 600 GHz
•Tapered coupling well thought out

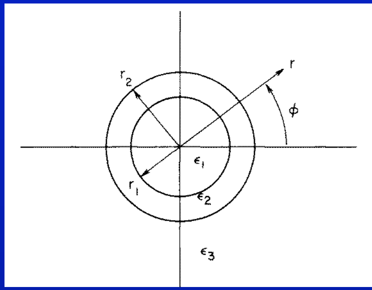

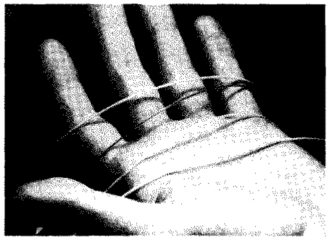

Fig. 6. Samples of W-band dielectric waveguide made by filling PTFE spaghetti with various low-loss dielectric powders.

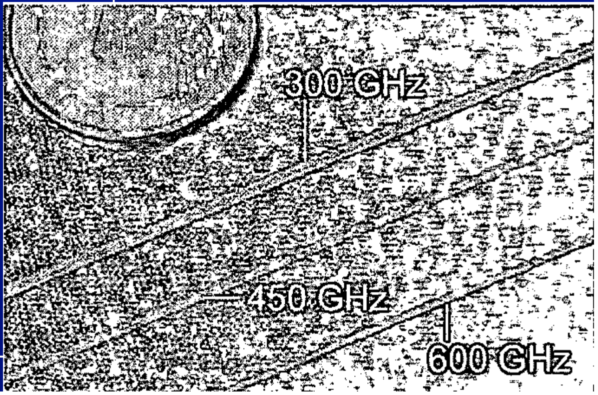

ULIRG evolution with redshift

From E. LeFloc'h
SPICA workshop Nov 06

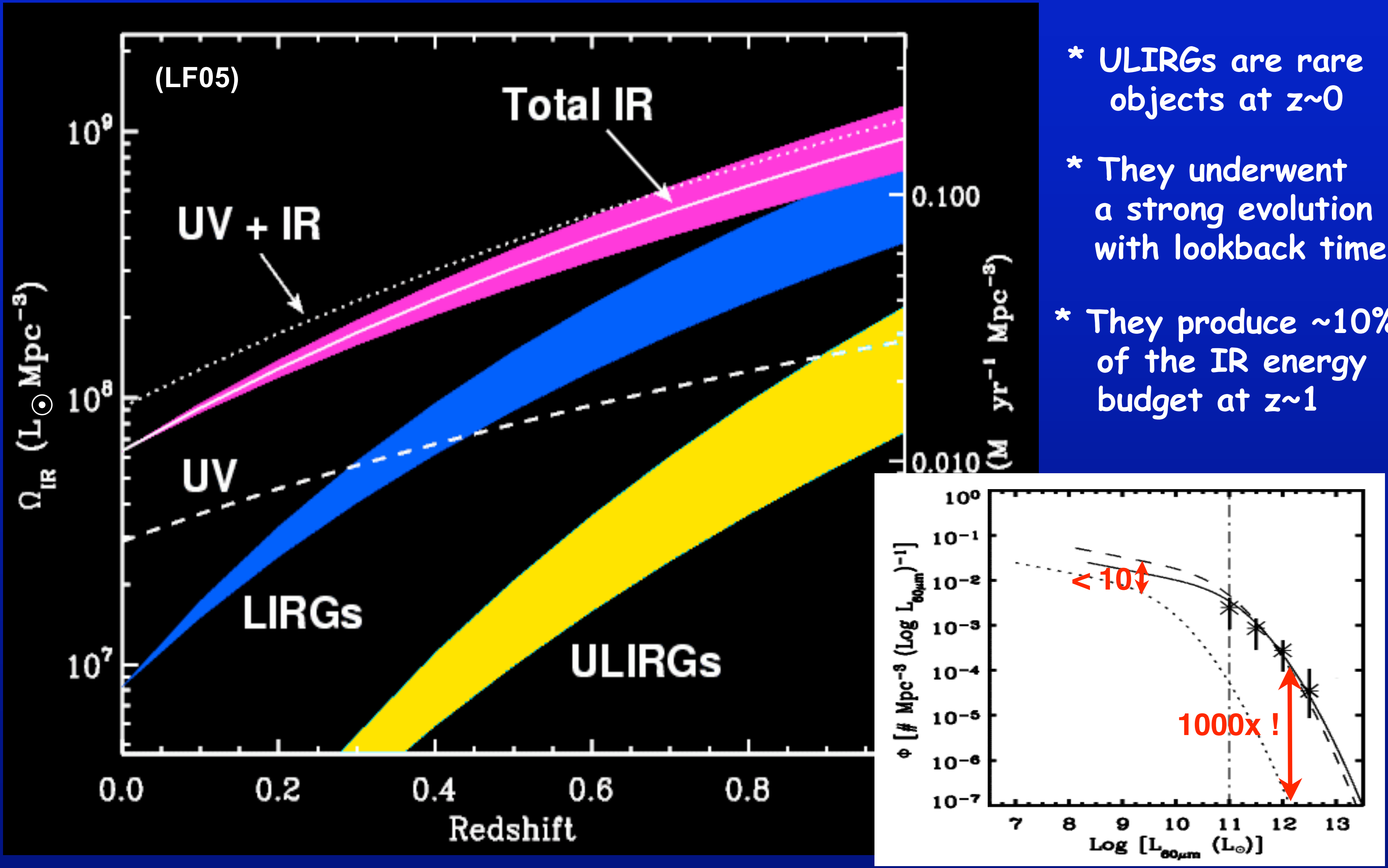

* ULIRGs are rare objects at z~0
* They underwent a strong evolution with lookback time
* They produce ~10% of the IR energy budget at z~1